J 20 419 F

A Publication
for the Radio-Amateur
Especially Covering VHF,
UHF and Microwaves

VHF communications

Volume No. 22 · Winter · 4/1990 · DM 7.50

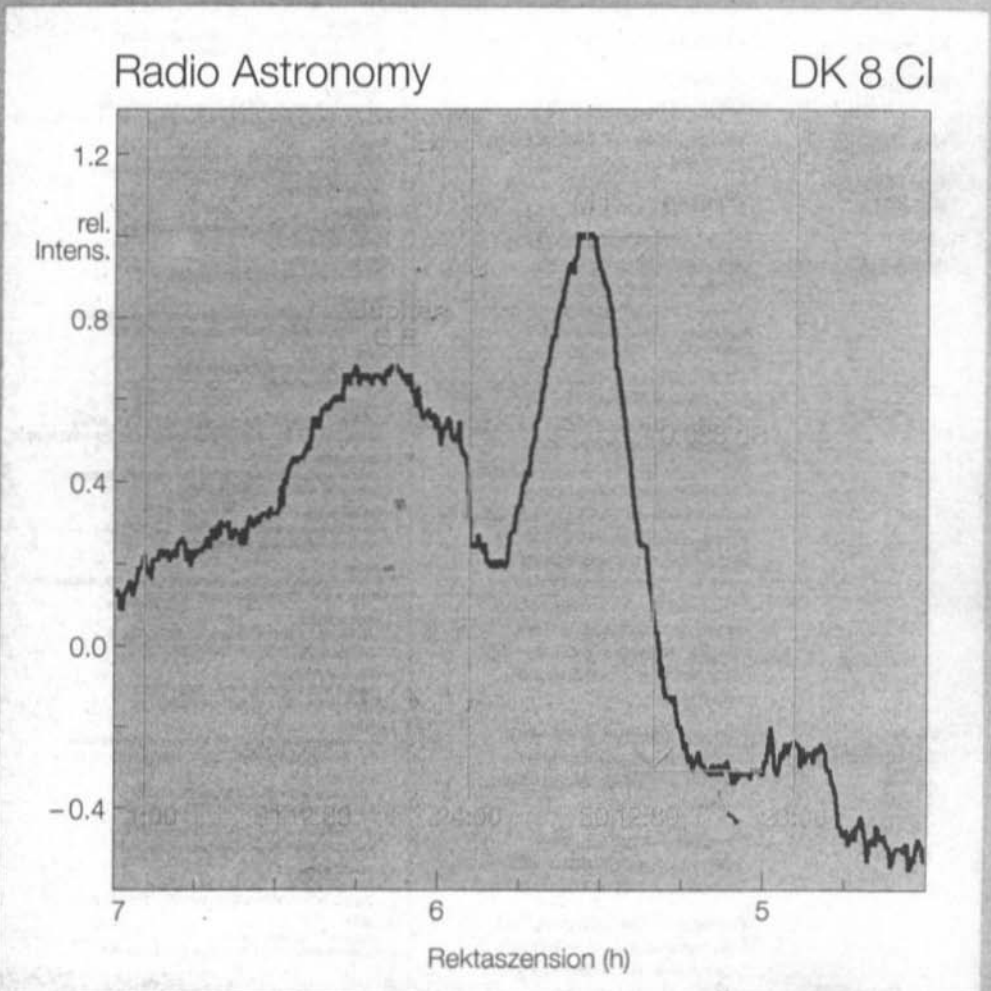

VHF communications

A Publication for the Radio Amateur
Especially Covering VHF, UHF, and Microwaves

Volume No. 22 · Winter · Edition 4/1990

Published by: TERRY BITTAN OHG, P.O.Box 80, Jahnstraße 14, D-8523 BAIERSDORF Fed. Rep. of Germany
Telephone (9133) 47-0 Telex 629 887
Telefax 0 91 33-47 47
Postgiro Nbg. 30455-858

Publishers: TERRY BITTAN OHG

Editors: Corrie Bittan
Colin J. Brock (Assistant)

Translator: Colin J. Brock, G 3 ISB/DJ Ø OK

Advertising manager: Corrie Bittan

VHF COMMUNICATIONS The international edition of the German publication UKW-BERICHTE is a quarterly amateur radio magazine especially catering for the VHF / UHF / SHF technology. It is published in Spring, Summer, Autumn and Winter. The 1990 subscription price is DM 27.00 or national equivalent per year. Individual copies are available at DM 7.50 or equivalent each. Subscriptions, orders of individual copies, purchase of PC-boards and advertised special components, advertisements and contributions to the magazine should be addressed to the national representative, or – if not possible – directly to the publishers.

Printed in the Fed. Rep. of Germany by R. Reichenbach KG Krelingstr. 39 · 8500 Nuernberg.

We would be grateful if you would address your orders and queries to your representative.

Representatives

Austria
Verlag UKW-BERICHTE, Terry D. Bittan
POB 80, D-8523 Baiersdorf / W. Germany

Australia
W.I.A. P.O. Box 300, South Caulfield, 3162 VIC,
Phone 5285962

Belgium
HAM TELECOM NV., Brusselsesteenweg 428,
B-9218 GENT, PCR 290-0148464-75,
Tel. 091/312111

Denmark
Halskov Electronic, OZ 7 LX, Sigersted gamle Skole,
DK-4100 RINGSTED, Tel. 53-616162 (kl. 19-22). Giro 7 29 68 00

France
Christiane Michèl, F 5 SM, SM Electronic,
20 bis, Avenue des Clairions, F-89000 AUXERRE
Tel. (86) 46 96 59

Finland
Peter Lytz, OH 2 AVP, Yläkartanonkuja 5 A 9
SF- 02360 ESPOO
SRAT, PL 44
SF-00441 Helsinki, Tel. 358/0/5625973

Holland
DOEVEN-ELEKTRONIKA, J. Doeven, Schutstraat 58,
NL-7901 EE HOOGEVEEN, Tel. 05280-69679

Israel
Doron Jacobi 4Z4RG, P.O. Box 6382
HAIFA, Israel 31063

Italy
ADB ELETTRONICA di Lucchesi Fabrizio, IW 5 ADB,
Via del Cantone 714, 55100 Antraccoli (Lucca), Tel. 0583-952612

Luxembourg
TELECO, Jos. Faber, LX 1 DE, 5 - 9, Rue de la fontaine,
ESCH-SUR-ALZETTE, Tel. 53752

New Zealand
E. M. Zimmermann, ZL 1 AGQ, P. O. Box 31-261
Milford, AUCKLAND 9, Phone 492-744

Norway
Henning Theg Radio Communication, LA 4 YG, Kjelaveien 30,
N-1370 ASKER, Postgirokonto 3 16 00 09

South Africa
HI-TECH BOOKS, P. O. Box 1142, RANDBURG,
Transvaal 2125, Tel. (011) 886-2020

Spain + Portugal
Julio A. Prieto Alonso, EA 4 CJ, MADRID-15,
Donoso Cortès 58 5°-B, Tel. 243.83.84

Sweden
Lars Pettersson, SM 4 IVE, Pl. 1254, Smégården Talby,
S-71500 ODENSBACKEN, Tel. 19-50223, Pg. 914379-3

Switzerland
Terry Bittan, Schweiz. Kreditanstalt ZÜRICH,
Kto. 469.253-41; PSchKto. ZÜRICH 80-54.849

Heinrich Dreher, HB 9 CKB, Elektronikvertrieb
Vormatt 2, CH-4463 Buus, Tel. 061-8412858

United Kingdom
Mike Wooding, G 6 IQM, 5 Ware Orchard
Barby, nr. Rugby, Warks CV23 8UF, Tel. 0788 890365

USA
Timekit, P. O. Box 22277,
Cleveland, Ohio 44122, Phone: (216) 464-3820

ISSN 0177-7505

Contents

Hermann Hagn, DK 8 CI Dr. Andreas Ulrich	**The Initial Results of the Garchinger Amateur Radio-Astronomy Installation**	194 - 201
Dragoslav Dobričić, YU 1 AW	**An Unconditionally-Stable, Low-Noise GaAs-FET Pre-Amplifier**	202 - 218
Matjaž Vidmar, YT 3 MV	**Amateur-Radio Applications of the Fast Fourier Transform Part 2b (Concluding)**	219 - 229
Detlef Burchard, Box 14426, Nairobi, Kenya	**A Short-Wave Receiver PLL**	230 - 243
G. Tomassetti, I 4 BER S. Mariotti, IK 4 JGD	**A "New" Feed for the 3 cm Band**	244 - 247
Wolfgang Borschel, DK 2 DO	**Tropospheric Forward-Scatter Propagation**	248 - 249
Jochen Dreier, DG 8 SG	**Simple Improvements to the DK 2 VF Microstrip Directional Coupler**	250 - 253

Farewell to our Readers

I regretfully announce that this will be the last edition of VHF COMMUNICATIONS to be published by Terry Bittan OHG. I would like to thank all our subscribers for their support during 22 years of the magazine's existence. I would also like to thank Colin (G3ISB) and his XYL for the effort of rewriting of the original UKW-BERICHTE articles into English. They are not professional translators, the work being sprung on to them following the tragic death of Terry Bittan in a light-aircraft accident six years ago. The detailed, and sometimes arduous, task of rewriting was undertaken in the spirit of a commitment to the constructional side of amateur radio and was therefore somewhat in the nature of a "labour of love" for G3ISB.

UKW-BERICHTE will continue to be published together with the sale of kits and parts associated with the articles and other ancillary equipment. Past editions of VHF COMMUNICATIONS are still available at reduced prices (see back cover page).

All subscriptions for VHF COMMUNICATIONS should now be sent to our UK representative **Mr Mike Wooding, 5 Ware Orchard, Barby Nr. Rugby, Warks CV23 8UF, Great Britain.**

I wish both you and the relaunched VHF COMMUNICATIONS all the very best for the future,

with sad 73s, **Corrie Bittan, editor**

UKW**berichte** T. Bittan OHG · Jahnstr. 14 · Postfach 80 · D-8523 Baiersdorf
Tel. 09133-47-0 · Telefax 09133-4747 · PSchKto Nürnberg 30455-858

Hermann Hagn, DK 8 CI and Dr. Andreas Ulrich

The Initial Results of the Garchinger Amateur Radio-Astronomy Installation

From a lecture at the VHF-UHF 90 Convention in Muenchen

This article is about the initial observations made by the Garchinger radio astronomy installation. The installation, which was erected in the grounds of the Munich Technical University, was originally conceived for the reception of the weather satellite METEOSAT 2. It was then modified following the interest aroused by DL2MDQ at the VHF-UHF 1988 (1) convention, so that a further receiver intended for radio astronomical observations could be connected.

1. ANTENNA

A Siemens type PS 3-2.2, 3 m-parabolic reflector serves as the reception antenna. The focal length is 75 cm and the −3 dB beamwidth 4.5°. It is mounted on a 6 m-high tubular, steel tower. The antenna is freely rotatable in the azimuth trough 360° and in elevation from 0 to 82°. Both plane adjustments are manual. During measurements, the antenna is locked into position, the astronomical sources to be observed then run through the antenna lobe according to the movement of the earth about its axis.

2. RECEIVING INSTALLATION

The receiving installation works in the frequency range around 1720 MHz. **Figure 1** gives an overall impression of the installation.

A waveguide feed system is located by means of λ/4 decoupler sections in the focus point of the parabolic antenna. The signal is taken to the first amplifier stage via a 20 cm (approx) semi-rigid cable. It works with a CFY 19 and has a gain of some 16 dB. Via a circulator, working as an isolator, it is taken to a second amplifier which gives it a further 20 dB of gain. The combined noise figure of both amplifiers with cable was measured at 1.3 dB at 1720 MHz.

The measurement test gear, near the foot of the tower, was connected to the receive pre-amplifier

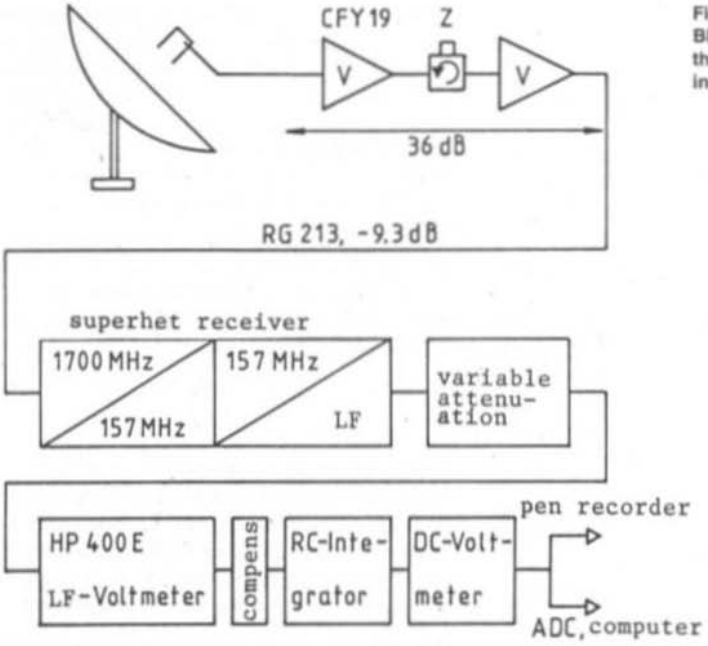

Fig. 1:
Block diagram of the complete installation

by means of a 26 m-long length of RG213 cable having an attenuation of 9.3 dB. The signal was then further processed by a surplus test receiver having a noise figure of 3 dB. This receiver has a switched, variable attenuator having 1 dB steps and a fine adjustment for the between values of output level. There are also two outputs available, one video of 1 MHz bandwidth, AM demodulation and the other a DC output. The receiver functions without AGC. Its LF output has a signal available which is always proportional to the antenna voltage. It is measured with a milli voltmeter (HP400E) which is connected via a stepped attenuator to the receiver output.

The output of the milli voltmeter delivers an auxiliary 0 to 1 V potential, which is proportional to the signal input, to a pen recorder. In the absence of a signal at the antenna, this DC voltage is determined only by the internal noise of the receiver. This portion is compensated and the rest amplified and taken to an integrator having a 10 s time constant (approx). The registration of the signal is carried out with an xt writer, but also at times, using a computer (Atari 1040 and Rhobus), via a 12 bit analog-digital converter (ADC).

3. INSTALLATION ALIGNMENT

In order that successful measurements of extremely weak radio emissions can be made, the installation must be optimally adjusted and its sensitivity calibrated in order that the various signal sources and interference signals can be measured. In this respect, it was extremely helpful that a known level of signal, at a convenient elevation, was available from the METEOSAT on 1695 MHz. At this position, the antenna tubular feed system was adjusted for maximal satellite signal strength.

At the same time, the radio-telescope receiver was tuned to a frequency 20 MHz higher. The received signal originates from the cold quarter of the sky in the direction of the satellite. The fine adjustment of the feed system is carried out by tuning for minimal background signal, as every defocusing movement will result in an increase in the radiation component from the immediate vicinity of the antenna.

The gain of the antenna, or more accurately, the illumination area (effective area) of the antenna, can also be determined with the assistance of the METEOSAT signal. The effective antenna area is an extremely important quantity as with a knowledge of it, one can determine the system's capability to receive a known astro-radio source. The ratio of the effective antenna area to its actual physical area is a measure of the efficiency of the parabolic antenna. The departure of this value from unity is dependent upon dish reflection losses, errors in focusing and the shadowing of the dish by the antenna feed system.

The antenna efficiency is determined by the following procedure:–

A signal generator is adjusted to obtain the same S-meter deflection as that received from the METEOSAT 2 satellite. Previously, the insertion gain of the antenna pre-amplifiers and the losses in the 50 Ω-connecting cables was measured using a commercial power-meter (Rohde & Schwarz URV5). Using this, the power received at the antenna terminals could be calculated to be 1.49×10^{-14} W. The known radiation flux from the satellite is 3.72×10^{-15} W/m^2 (−144.3 dBW/m^2). This works out to an effective area of 4 m^2 which is 57 % of its physical area.

A further parameter which can be measured is the intrinsic noise of the system. This can be expressed in dB, kT_0 or as a noise temperature T_e in Kelvin. These quantities are related to one another in the following manner:–

$$F(dB) = 10 \log (kT_0)$$

$$F(dB) = 10 \log (1 + T_e/290)$$

In this case, the noise figure of the overall electronics was measured with a calibrated noise generator at 1.3 dB, i.e. 100 K. This value is identical with the noise figure of the pre-amplifier since, owing to its high gain, the second-stage contribution of the receiver itself, is insignificant.

The conclusion to be drawn from the measurements described, is that the atmosphere and also, possibly, the trees in the vicinity, additionally contribute 65 K to the noise at an antenna elevation of 40°. Altogether, the system noise temperature (2) is about 165 K at antenna elevations over 40°.

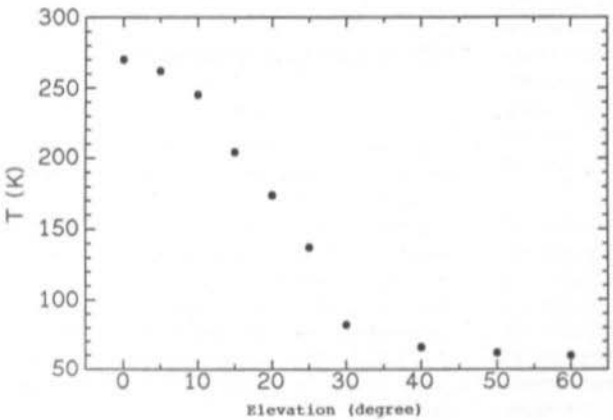

Fig. 2:
The antenna temperature as a function of elevation. Only at elevations over 40° is the contribution from the antenna environs negligible. All astronomical measurements were made at above 35°.

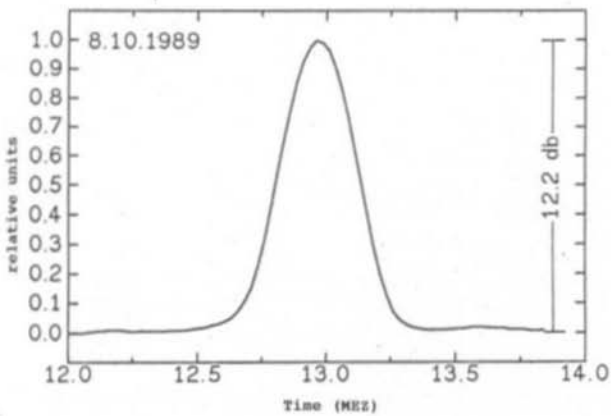

Fig. 3:
Typical progression of the Sun

4. ANTENNA TEMPERATURE

The antenna was turned to a horizontal position (elevation 0°) on a clear day at an outside temperature of −3° C. The signals measured at the receiver output came exclusively from the immediate environment of the antenna which corresponded to their physical temperature of 270 K. When the antenna was then raised in elevation the signal strength decreased as depicted in **fig. 2**. The signal decrease △S in dB is given by:–

$$\triangle S = 10 \log (270 + T_{rx})/(T_{rx} + T_{el})$$

where

T_{rx} = The received noise temperature
T_{el} = The system noise temperature at that elevation

In the search for extra-terrestrial noise sources at 1720 MHz the following objects were observed:

1. The Sun
   The signal power rose to 12.2 dB above the system noise temperature (in a cold, noise-free part of the sky) from 165 K.
2. The Galactical equator (constellation Archer) with a rise of 0.15 dB.
3. The Moon with 0.04 dB
4. The Orion Nebulae with 0.01 dB
5. The Galactical equator (Orion) with 0.05 dB
6. The Crab Nebulae with 0.036 dB
7. Jupiter with 0.01 dB

Observing the Sun presented no problems at all. A very nice transit of the Sun is shown in **fig. 3**.

The part of the Galactical equator only gives usable results with 50 % of all experiments. **Fig. 4** gives an example.

The emissions from the Orion Nebulae at 37° elevation are, however, much more difficult. The curve shown in **fig. 5** consists of summed values taken over a period of eight nights (the 8th, 10th, 13th, 14th, 17th, 18th, 20th and 21st of November 1989).

The Moon is usually recordable, especially at elevations around 50°. The observations are nearly always accompanied by atmospheric perturbations. The transit shown in **fig. 6** was exceptionally undisturbed and impressive.

Measurements in the Galactical equator in the region of Orion are at the limits of detectability

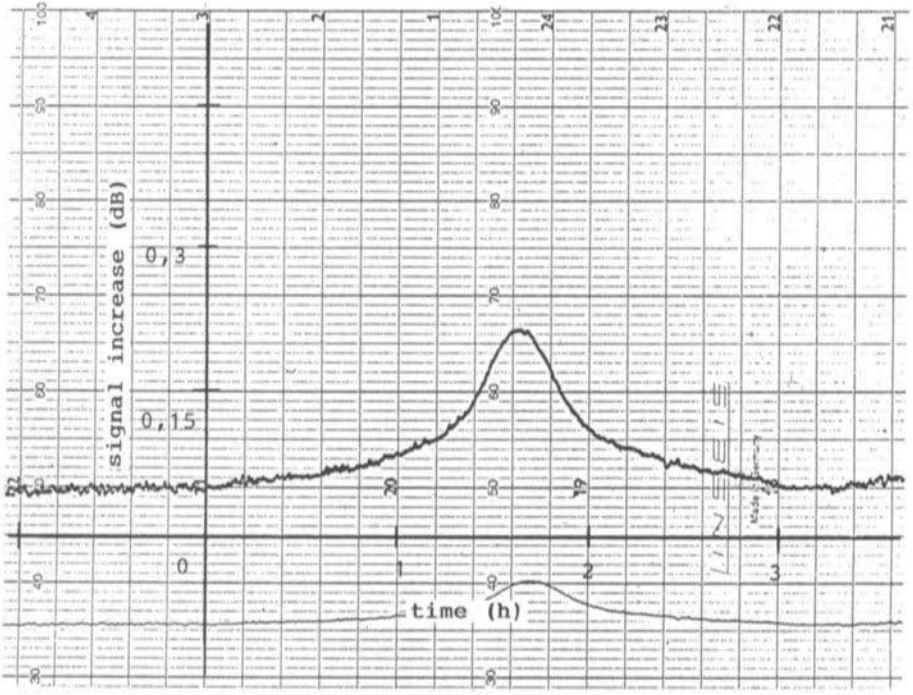

Fig. 4: Galactical equator near the constellation of the Archer. The signal represents an antenna temperature of 5 K. The noise amounts to some 0.1 K and the transition took 5 h.

of the installation at this time. The Crab Nebulae M1 (remnants of the Supernova observed by the Chinese) can be seen very clearly, **fig. 7**. The elevation is 65°.

Jupiter will be observable from December 1989 to January 1990 in the Galactical equator (constellation Twins) and appear in the antenna about 40 minutes after the Crab Nebulae. Normally,

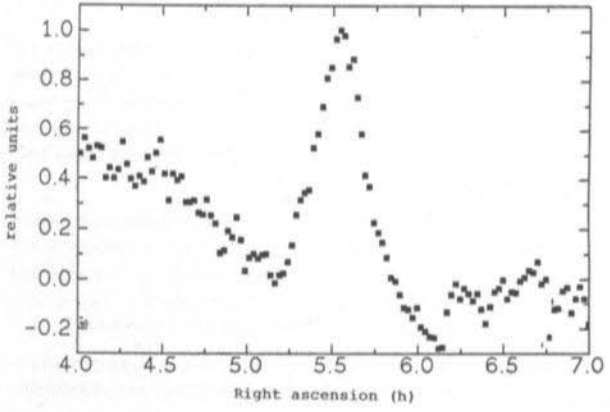

Fig. 5:
The Orion Nebulae. Because of the extremely weak signals at the relatively small elevation of 37° a total of eight transitions had to be made and the results summed.

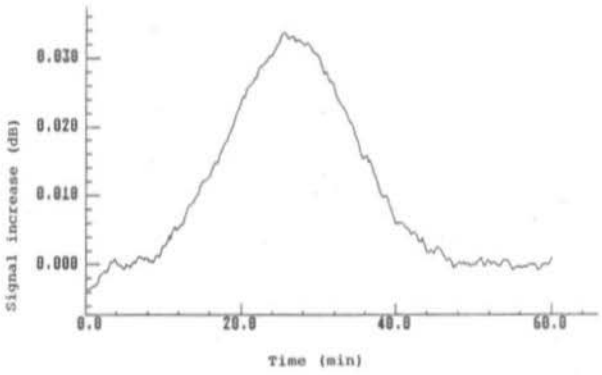

Fig. 6:
A Full-Moon transition

the signals from the Galactical equator and Jupiter are superimposed upon the Crab Nebulae. In two days, however, these signals increased dramatically (**fig. 8**). Bursts could also be observed which were reported in the literature as only for the meter-wave band. The signal had a peak value of 0.18 dB above the reference level of 165 K.

5. CONCLUSIONS

By means of simple deduction, the flux of some of the sources can be determined from their signals.

For this, the following formulae (1, 2) are employed:

$$T_a = SA_e/k$$

where: S is expressed in $W/Hz/m^2$
A_e in m^2

The unit for S has been internationalised to the Jansky (Jy). One Jy = 10^{-26} $W/Hz/m^2$.

$k = 1.38 \times 10^{-23}$ J/K (k = Boltzmann's constant)

The increase in signal in dB is expressed as the antenna temperature T_a and the system temperature T_{sys} and is given by:

$$\triangle S = 10 \log (T_a + T_{sys})/T_{sys}$$

1. For the Crab Nebulae, an increase in signal of 0.036 dB was measured. This gives an antenna temperature of T_a = 1.37 K, or a flux of

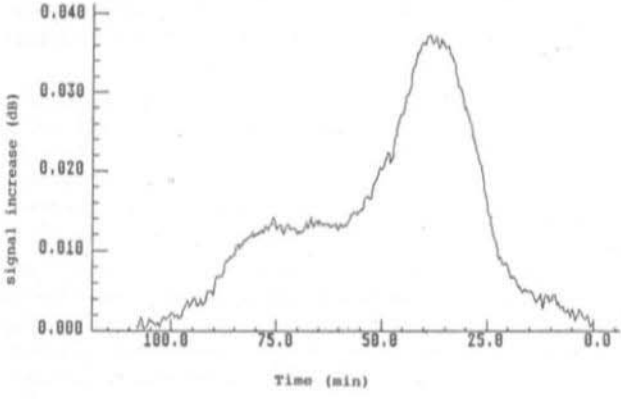

Fig. 7:
Crab Nebulae (large signal right) with the galactical equator by the constellation Twins and Jupiter (left)

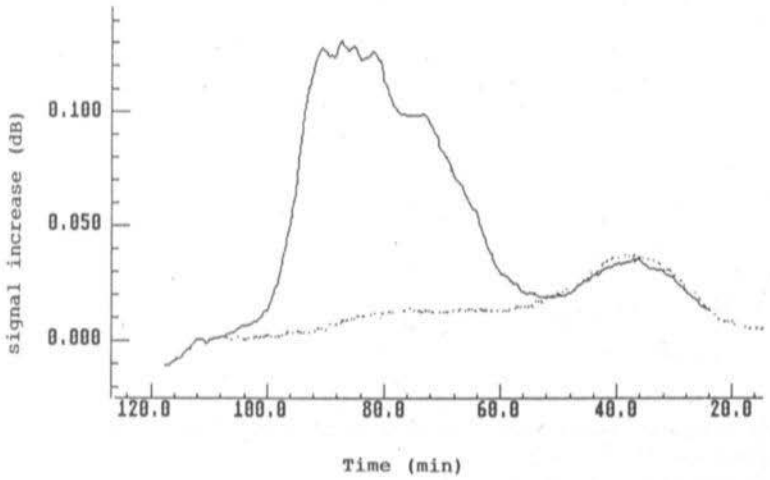

Fig. 8: As fig. 7 (dotted curve) but with a pronounced burst from Jupiter

473 Jy. As only one polarisation plane was observed, the total flux is twice as high. This agrees very well with the published values.

2. The Moon had an increase of 0.04 dB. This results in a T_a = 1.53 K, or 527 Jy. The Moon has a subtended angle of some 0.5° and the beamwidth of the antenna is 4.5°. From this, the radiation temperature of the Moon can be determined as follows:

$$T_{Moon} = 1.53\ (4.5/05)^2 = 123.9\ K$$

Again, the measurement was made in one plane only and therefore the results must be doubled. The radiation temperature of the Moon is made up of the inherent body temperature of the Moon and the reflected light of the Sun from its surface. The signals are therefore dependent upon the Moon's phases. The measurement shown was taken at full moon.

3. The Sun's measurement indicated a 12.2 dB signal increase. A typical measurement made during the year 1988 lay some 3 dB lower. The measured flux at the moment is in the region of 1.77×10^6 Jy. This result lies between the values for the Sun when active to when it is quiescent.

These measurements show that it is possible to achieve very good results using only modest equipment (3). The occasional mistakes, however, should not go unmentioned. The highest attention must be paid to the smallest temperature drift of the overall system. This confines all measurements (except those of the Sun, of course) to be made at night. The fact that the instruments were located in a cellar was helpful in this respect.

The measurement programme at 1720 MHz has now come to an end for the time being. The installation has been retuned to 1420 MHz – the frequency of the neutral hydrogen atom spectral emissions.

Further observations will be made using a 4.5 m diameter reflector which Siemens has placed at our disposal. The beamwidth of this antenna at 11 GHz is only 0,3°. Observations will be mainly carried out on 2.7 cm and the initial subjects will be the Moon, Jupiter and the Sun.

Incidently, a transitional X band has been constructed on a circular waveguide, as now EME on 10 GHz will then be possible – the antenna having a theoretical (!) gain of some 53 dB which borders on the very limit of feasibility. The trans-

mitter here has 100 W power output at 10 GHz giving a radiated power of some 20 MW (!).

mit einer 3-m-Parabolantenne
Erscheint in „Sterne und Weltraum" 1990

6. REFERENCES

(1) Hartfuss, Hans J.: Radio Astronomy for the VHF/UHF Radio Amateur
VHF COMMUNICATIONS Vol. 21, Ed. 4/1989, P. 194 - 204

(2) Vowinkel B., Hartfuss H.J.:
Passive Mikrowellen-Radiometrie
Verlag vieweg, Braunschweig 1988

(3) Andreas Ulrich, Hermann Hagn:
Beobachtungen im Radiobereich bei 1,7 GHz

The following books were of great assistance during the construction and operation of the installation;

John D. Kraus: "Radio Astronomy",
Verlag Mc Graw-Hill, New York 1966

Joachim Hermann: „dtv-Atlas zur Astronomie",
Deutscher Taschenbuch Verlag, München, 1985

To all who have assisted in this project with both advice and physical labour, we would like to extend our grateful thanks. They are as follows:– Max Münich, DJ1CR, Bernd Weiß von der TU München, Dr. Hans Hartfuss, DL2MDQ und Knut Brenndörfer, DF8CA.

Dragoslav Dobričić, YU 1 AW

An Unconditionally-Stable, Low-Noise GaAs-FET Pre-Amplifier

The appearance of the GaAs-FET with its extremely low-noise figure at very high frequencies, has led to the wideband belief that all problems of constructing low-noise pre-amplifiers have been solved. That, unfortunately, is not the case. Because these devices were designed to provide high gain at SHF, attempts to construct amplifiers at frequencies below 2 GHz is a very serious undertaking.

The success in their employment depends upon the solution of a few problems, each of which requires careful consideration and a planned approach. They are as follows:–

1. **A very low-loss input circuit and very good matching to the transistor is essential for a good noise-figure. The optimum impedance for the lowest noise will be very high and have a reactive component, which will make this quite difficult.**
2. **Almost all GaAs-FETs exhibit unconditional stability at frequencies above 4 GHz and their operation at lower frequencies is attended by a significant tendency to self-oscillate. Owing to the high gain and only conditional stability at the lower frequencies, it is very difficult to design and build a really stable amplifier (6).**
3. **Because of the conditional stability and that over only a very limited range of impedances, the output matching of the transistor is very critical. This tends to result in an improperly tuned amplifier together with a poor performance.**

1. MATCHING FOR OPTIMUM INPUT

The problem of the input matching, that is, achieving the lowest noise figure together with minimum input ciruit losses, has been discussed in (1). The salient points arising were:–

1. The input tuned circuit matching the antenna to the input of the active device must have the highest possible unloaded Q (Q_U).
2. The matching circuit must be so dimensioned that it has the lowest-possible loaded Q (Q_L).

For the 2-metre band, a helical resonator should be provided since it possesses a Q_U of double that of conventional LC-tuned circuits, as discussed in (1).

At 432 MHz and higher frequencies, the best solution is the use of a coaxial resonator for the input circuit but air-insulated, stripline resonators have quite a high Q_U and are acceptable for this purpose.

Resonator losses are directly proportional to the circulating currents and to keep these low, the dimensions of the resonator are important. Both the inner and the outer diameter and their ratio are factors for attaining a maximum Q_U and thereby minimum losses (2).

The unloaded Q of a coaxial resonator, made from copper or silver, can be evaluated by means of the following formula:–

$$Q_u = D * \Theta * \sqrt{f} \qquad (1)$$

$$\Theta = 151 * \frac{\ln (D/d)}{1 + D/d} \qquad (2)$$

where,

D = outside diameter (cm)
d = internal diameter (cm)
f = frequency (MHz)

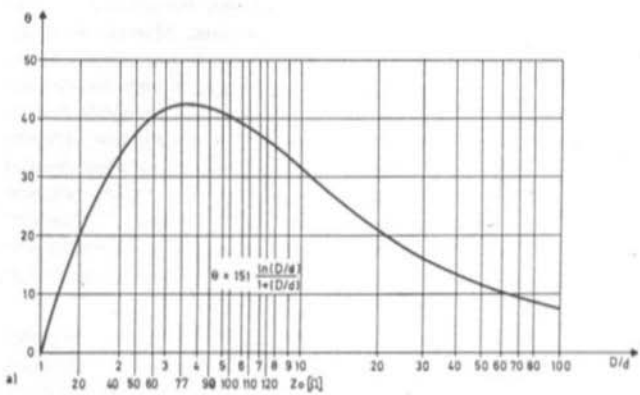

Fig. 1a:
θ Value for coaxial resonator, in dependance of D/d ratio of characteristic impedance Z_o

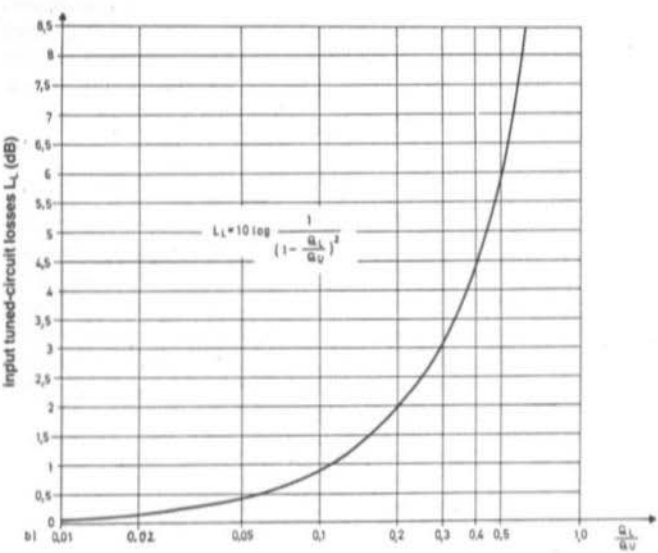

Fig. 1b:
Input resonator loss L_L in dependance of Q_u/Q_L ratio

The values of Q_U calculated from this formula conform very well to those measured in practice.

Equation (1) indicates that the unloaded Q at any given resonator diameter and frequency will be a maximum when Θ has a maximum. The equation (2) for Θ, in turn, has a maximum value when D/d = 3.6 as shown in **fig. 1a**.

From the well known formula for the characteristic impedance of a coaxial resonator:–

$$Z_O = 60\ L_n\ (D/d)..(\Omega)$$

and plugging in 3.6, a resonator Z_O of 77 Ω is obtained.

The resonator having the highest possible unloaded Q must have silvered surfaces, a characteristic impedance of 77 Ω and as large a diameter as possible. When the side of a square resonator has the same dimension as the diameter of a round one, then Q_U will be some 20 % higher.

The next task is to calculate the impedance transformation for the input circuit under the minimum working Q (Q_L) conditions.

In order that the antenna impedance of $R_L = 50\ \Omega$ is transformed with the optimum impedance for the lowest noise-figure of the transistor:

$$Z_{NF} = R_{NF} \pm jX_{NF}$$

the input tuned circuit must have a Q_L which is higher than two certain minimum values, Q_M and Q_D. Both these minimum values of Q_L will be determined by the impedance Z_{NF}.

$$Q_M = \sqrt{\frac{R_{NF}}{R_L} - 1}$$

$$Q_D = X_{NF}/R_{NF}$$

The Q_L of the input circuit should be higher than Q_M and Q_D, or at least, be equal to the value of the higher of the two. The importance of the impedance Z_{NF} for the final results and for the choice of a suitable transistor is now clear.

Finally, it is now possible to calculate the loss in the coaxial resonator:

$$L_L = 10\log\ \left(\frac{1}{1 - Q_L/Q_u}\right)^2 \qquad (3)$$

The electrical loss in a resonator L_L, in dB, for a given ratio Q_L/Q_U is shown in **fig. 1b**.

Besides the resonator, the input circuit comprises tuning and loading capacitors and the losses in these can be calculated in a similar fashion, if their respective Q_Us are known for the frequency of operation. Alternatively, the use of known high-quality components will ensure a negligible loss.

The main losses in capacitors at high frequency are caused by skin effect, dielectric absorption, resistance of sliding surfaces in trimmers and losses in the component constructional insulating material. If, however, silvered plate capacitors having air-dielectric and without sliding surfaces are used, the loss is very low indeed. A capacitor of this type can be easily formed by using two plates and moving one of them. This type of trimmer capacitor is often used in UHF tube power-amplifiers having stripline resonators. The very expensive "Johanson" trimmers are very high-quality components with Qs of a few thousand at frequencies below 1.5 GHz.

The capacitance value of a tuning capacitor C_t connected across the input of the transistor must be very low. A high value of this capacitor would increase Q_D and also decreases the LC-ratio of the input circuit, thus lowering its dynamic resistance R_D. As a consequence, higher losses and higher noise-figure are to be expected. The noise-factor F at the transistor's input can be expressed by the following equations:

$$F = 1 + R_{NF}/R_D \qquad (4)$$

$$R_D = Q_U * X_L = Q_U * X_C \qquad (5)$$

Almost all GaAs-FETs below 1.5 GHz have a high value of R_{NF} and it could easily occur that an injudiciously chosen, lower value of R_D has the same order of value as R_{NF}. This could result in the noise figure being increased by 3 dB even before the transistor's noise figure has been taken into account (3).

In conclusion, for optimum input matching and to achieve the minimum noise and loss, the following rules must be observed:

1. Use resonators with the highest possible Q_U.

2. The Q_L of the input tuned-circuit must be as low as possible but higher than Q_M and Q_D.

3. The tuning capacitance C_t must be as low as possible, just sufficient to ensure a positive tune. The L/C-ratio of the input circuit must be held as high as possible.

2. STABLE OUTPUT MATCHING

Matching a transistor output for stable working conditions is usually much more difficult than optimum input matching. The output matching has no influence on the noise-figure as almost all GaAs-FETs below about 1.5 GHz have a scattering parameter S_{12} of practically zero. **The transistor's output matching, however, is of paramount importance for its gain and stability.**

As already mentioned, most GaAs-FETs are only conditionally stable below frequencies of around 4 GHz. The stability-factor calculations and the superimposing of stability and constant-gain circles onto the Smith Chart will present a clear picture of the problem to be solved, **see fig. 2**.

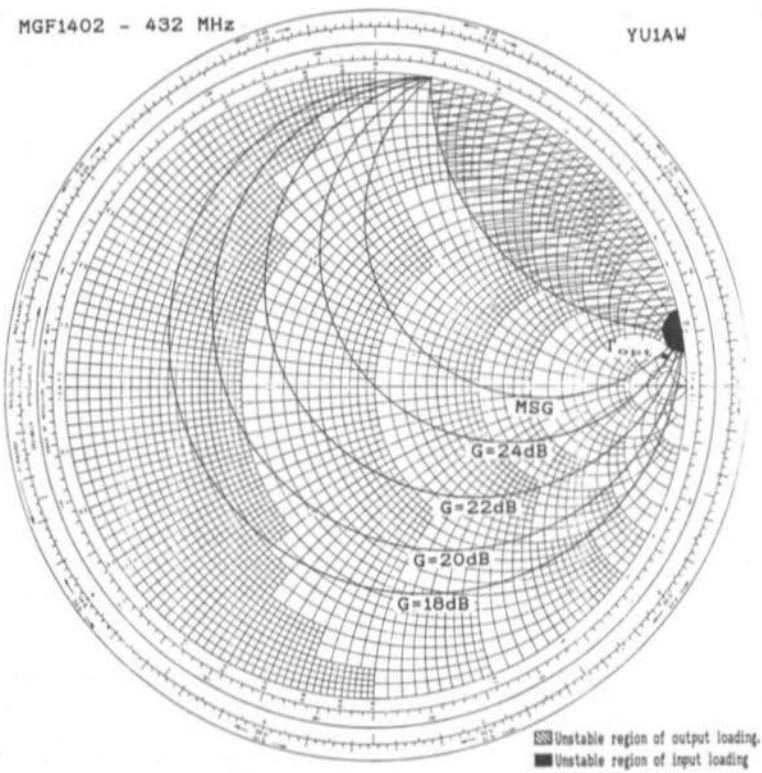

Fig. 2: Stability and constant gain circles for MGF 1402 on 432 MHz, with given unstable regions of input (black) and output (lined) impedances

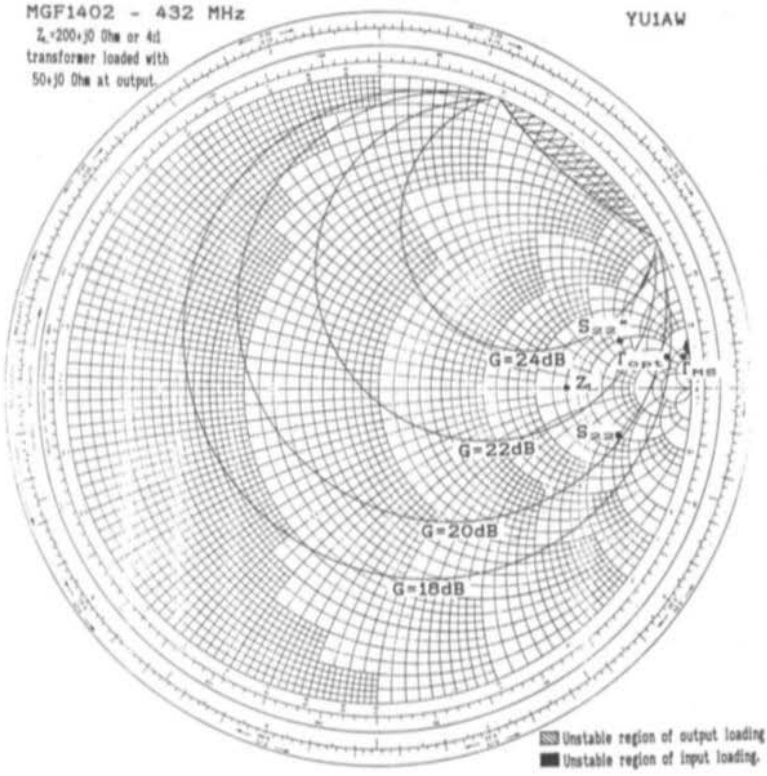

Fig. 3: Constant gain and stability circles for MGF 1402 on 432 MHz, loaded on output with transformer 4 :1 or resistor 200 Ω

Many constructors have come across this problem and have tackled it usually by using either a resistive output load (1) or 4 : 1 ferrite transformers (6). Following these concepts, many preamplifiers have been constructed and published but undoubtedly were only conditionally stable over a certain range. The Smith Chart of **fig. 3** shows the conditions when a 4 : 1 transformer is connected to the output or loaded by a 200 Ω resistor. The construction confirms that the transistor is only conditionally stable.

This means that the amplifier, when subjected to certain output load conditions and input source admittance, will self-oscillate. This critical condition can occur very easily, for instance, when two amplifiers are cascaded and the pre-amplifier has been loaded by an impedance which has been transformed by a 4 : 1 transformer. The transformers are usually wound on a ferrite core, or bead, whose permeabilities are not known above a few hundred megahertz.

Many of these transformers having various sizes, types of core, number of turns and winding diameters have been checked by a network analyzer. All examples of this type of transformer displayed a very high reactive component of input or output impedance when terminated by a resistive load (7).

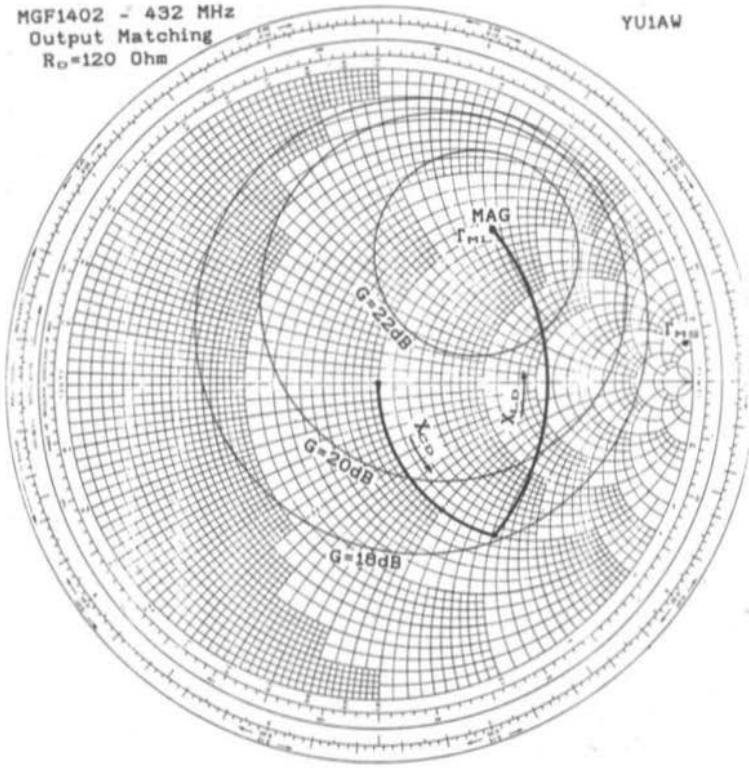

Fig. 4: Constant gain circles and the way of output matching of MGF 1402 on 432 MHz with shunt-resistor R_D = 120 Ω and high-pass L matching network, as suggested in text. Amplifier is unconditionally stable and with aid of reactances of coil X_{LD} and capacitor X_{CD} it is very easy to achieve max. gain (MAG)

It must therefore be concluded, that these transformers perform very poorly, even at frequencies in the 2-metre band, and introduce stability problems because of their high component of reactance. The resistive loading has therefore the advantage that it enables stable operation over a much wider range of output impedances but fig. 3 makes it clear that the transistor will self-oscillate over quite a large range of inductive impedances.

Quite apart from the problem of stability, there is the potentially even more difficult problem of output matching (4). This can mean that the amplifier presents a very poor source impedance to the following stage. It is left to the imagination what will happen if two conditionally-stable amplifiers are connected in cascade – either a two-stage oscillator is created, or an amplifier which is working well below its potential performance.

It may be concluded that the output matching of GaAs-FETs working at low frequencies is not an easy task to solve. Every constructor's aim is to build an unconditionally-stable amplifier with high gain, extremely low noise and a low output VSWR.

The design presented in this article will go a large way in realizing this objective.

3. CALCULATING FOR UNCONDITIONAL STABILITY

The characteristics and behaviour of a transistor at a specified frequency, are defined by scattering, or S-parameters. The use of these parameters enables many important values to be revealed:–

1. The stability factor K is a measure of the transistor's tendency to oscillate. When K is greater than unity, the transistor is unconditionally stable, that is, the connection of any passive load or source admittance will induce oscillation.
2. The Maximum Stable Gain (MSG)
3. The Maximum Available Gain (MAG). This is the forward power gain when the input and output are simultaneously, conjugately

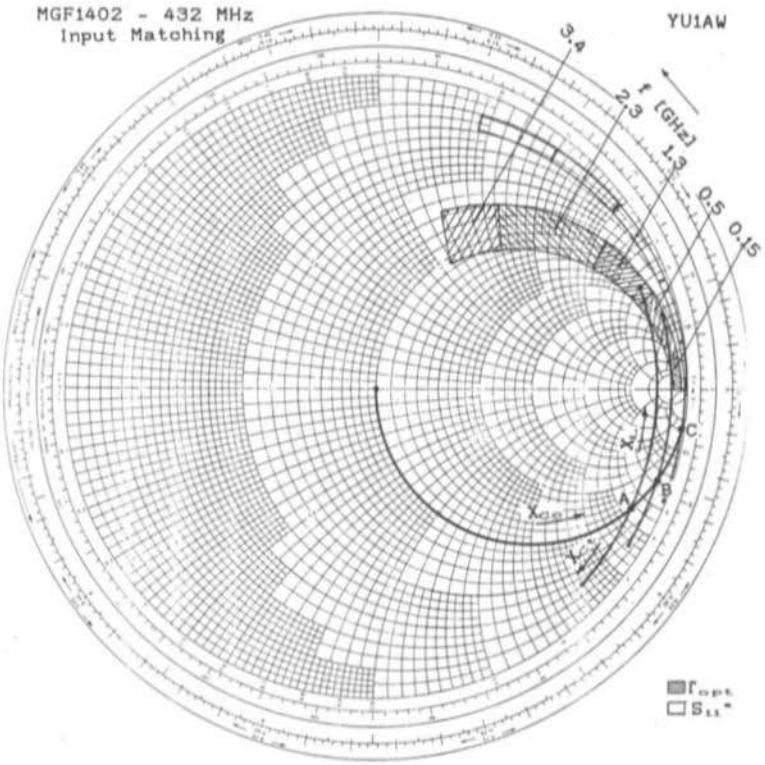

Fig. 5: Input matching of MGF 1402 on 432 MHz with aid of reactances of coil X_L and capacitors X_{Ce} X_{Ci} to minimum noise or maximum gain.

matched. The MAG is only defined for a device which is unconditionally stable (K > 1).

A conditionally-unstable device may be made stable by connecting a resistive load at its output. As it has already been seen, however, it is not possible to use just any value of load resistance as the device can remain unstable or even start oscillating. The resistance value must be determined by calculating the new S-parameters of the device together with the resistor-cascaded network (4). From the S-parameters, the stability factor K can be determined. When K is greater than unity, the value of resistance has been found which will make the amplifier unconditionally stable (4). After the value of the shunt resistance has been found using the new S-parameters, the input and output reflection coefficients for the maximum available gain (MAG) can be found (5). See fig. 4.

The value of the gain obtained for the MAG is smaller than of the MSG of the potentially unstable device before the addition of the shunt resistor, but it nevertheless represents a good trade-off. A few dBs of gain has been sacrificed in order to make the amplifier unconditionally stable. High frequency GaAs-FETs also have a very high gain at lower frequencies and there is still sufficient gain left.

The output matching for MAG is accomplished by the use of a high-pass L-network. This circuit will achieve simple and effective matching together with DC-blocking whilst using the minimum number of components. **Fig. 6**.

The MAG for the majority of GaAs-FETs is around 20 - 22 dB, lower than the MSG about 2 - 5 dB depending upon type and frequency. As mentioned previously, the MAG is achieved under conditions of a simultaneous, conjugate match of input and output. But, an input match for minimum noise and not the maximum amplification, is what is required. The input match for minimum noise entails a gain of around 2 - 3 dB lower than MAG.

The output return-loss is about 40 dB (VSWR = 1.02 : 1) which is much higher than that achieved by using a 4 : 1 transformer or a resistive output load (VSWR = 3.5 : 1).

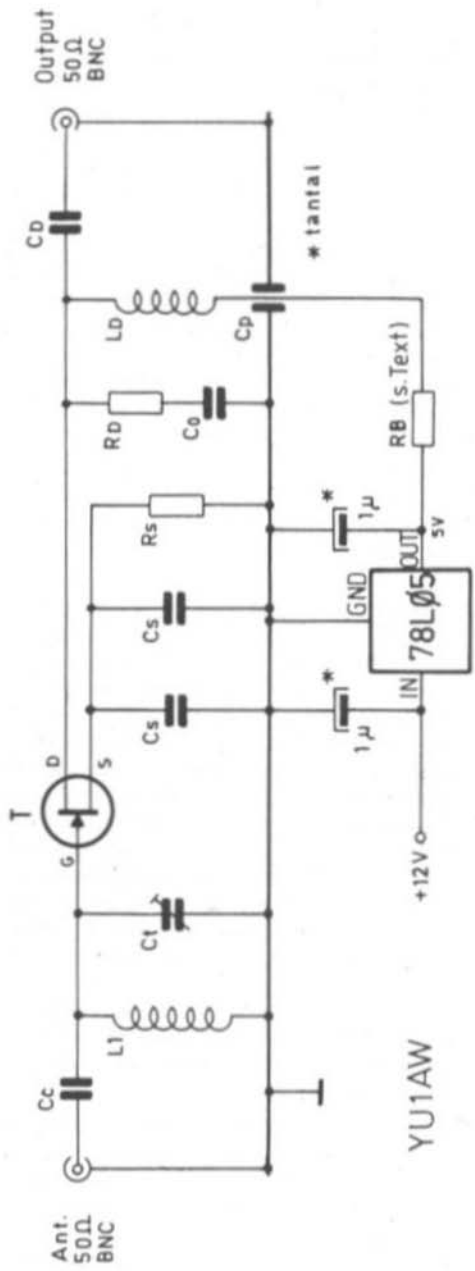

Fig. 6: Schematic diagram of unconditionally stable GaAs-FET preamplifier for 144 MHz

4. INPUT CIRCUIT CALCULATION AND TUNING

Almost all GaAs-FETs below about 4 GHz, have a high input impedance with a large capacitive component. Conjugated values (marked with *) of input reflection-coefficients S_{11} are shown on the Smith Chart in **fig. 5**. The optimum input reflection-coefficient for minimum noise Γ_{opt} or impedance Z_{NF} is also shown on the same Smith Chart. It may be readily concluded, that the reflection coefficients S_{11}^* and Γ_{opt} are similar in phase but differ in amplitude.

This fact can be used to tune the amplifier input tuned-circuit for minimum noise in a simple but precise manner without the use of instruments.

The transformation of the antenna impedance $R_L = 50 + j0$ to the optimum noise-figure impedance Z_{NF} using input circuit components C_t, C_c and L_1 (fig. 6) are given on the Smith Chart of fig. 5. Capacitor C_c transforms to the real part of the impedance R_{NF} whilst C_t together with inductance L_1, set the imaginary part of the impedance X_{NF}. From fig. 5, it is quite clear that different values of C_c, i.e. reactance X_{Cc}, will have a direct influence on whether the input matching will be for maximum power gain or for minimum noise. If the value of C_c is low, i.e. high X_{Cc}, the transformation will be on the line, Smith Chart centre (point C) and the amplifier will be tuned for maximum power gain. If, however, C_c is lower, i.e. lower X_{Cc}, then the transformation will be on the line, Smith Chart centre point (B or A), and consequently the amplifier will be tuned for minimum noise.

Thus, in order that the amplifier be tuned for minimum noise, it is necesary that the value of capacitor C_c be determined. Once this is established and fixed, the amplifier will be automatically adjusted for minimum noise and an adjustment of C_t will only result in a variation of the power gain. The power gain so attained, is some 2 to 3 dB lower than if C_c had been adjusted for a maximum gain MAG. This is normal and is the small price that must be paid to obtain the minimum noise figure.

For illustration purposes, **table 1** contains various values for the input circuit elements together with the consequent values of Q_L and input circuit losses. The calculations were made for different antenna matchings. It may be readily seen that with an accurately determined value for the coupling capacitor C_c no mis-tuning is possible, even under conditions of high antenna VSWR. Moreover, there is a wide range between points A and B on the Smith Chart for which minimum noise is possible and this allows a tolerance of some ± 20 % in the value of C_c making it relatively uncritical.

This begs the question of what is actually critical since there are many examples of poorly designed amateur preamplifiers in operation! The answer is rather simple and logical: for the amplifier described in this article all elements were optimized and very carefully calculated in order that no performance degradation will occur when a reasonable degree of component tolerance is adhered to. This, however, is not valid for any poorly designed amplifiers of the type mentioned earlier.

Another reason for poor performance is that the amplifier has been tuned to minimum noise literally by ear and this is always misleading. There will always be amateurs who will believe that the prerequisite for a good pre-amplifier is an extremely high gain. This misconception can lead to the lowering of the value of C_c to obtain the maximum possible gain (MAG). This is the sort of result which can be arrived at when the amplifier is tuned by ear and without the use of instruments. It really is difficult to convince some people, that the amplifier must be detuned in order to improve reception – but that is the fact of the matter.

5. A 144 MHz GaAS-FET PREAMPLIFIER

The preamplifier described here is a modified version of that described in the author's earlier

VSWR	Tuning for	C_t pF	C_c pF	Q_L	Input-circuit losses
1,0	min. noise	1,5	1,3	8,5	0,04 dB
	max. gain	2,4	0,7	49,3	0,16 dB
1,2	min. noise	1,2 - 1,5	1,2 - 1,4	8,5	0,04 dB
	max. gain	2,4	0,6 - 0,8	49 - 51	0,17 dB
1,5	min. noise	1,1 - 1,6	1,1 - 1,6	8 - 10	0,04 dB
	max. gain	2,3 - 2,5	0,5 - 0,8	48 - 53	0,18 dB
1,8	min. noise	1,1 - 1,6	1,0 - 1,7	8 - 10	0,04 dB

Table 1: Component values for the 432 MHz input tuned-circuit, its Q_L and losses in relationship to the antenna VSWR and the tuning objective

article on the subject (1). This had been designed as a conditionally stable amplifier with resistive output loading, an RF choke to feed in the DC-supply and a capacitor for DC-blocking. The modification to that circuit represents a further development and entails making it unconditionally stable in the afore-mentioned manner.

A third capacitor C_c, for DC-blocking of R_D, has been added to the two existing chip capacitors C_s soldered to the screening wall. All components together with their values are given in **table 2** and the ciruit schematic is shown in fig. 6. The amplifier's method of construction is given in the three sketches of **fig. 7**. No changes have been made to the helical-resonator, input circuit. This is effected with 5 turns of 2 mm silvered wire wound on a 18 mm-long, 13 mm-diameter forming tool. This inductor (1) has always proved itself very effective in practice.

The only modification concerns the coupling capacitor C_c which replaces the trimmer capacitor connected to the 3.3 pF ceramic disc. This is the fixed capacitor mentioned earlier which enables the amplifier to be tuned easily for minimum noise. The earlier inclusion of a ferrite bead was dropped on the grounds that it made the amplifier conditionally stable.

Trans. Type	f MHz	G_{max} dB	Stab.-F. K	loss dB	C_t pF	C_c pF	R_D Ω	C_D pF	L_D nH	D_D mm	l_D mm	n_D Turns
MGF 1200 *	144	20	+ 1.2	0.13	2.5	3.3	68	22	44	3	6	5.5
MGF 1200	432	19	+ 1.2	0.04	1.5	1.3	60	8.2	13	3	4	2.5
MGF 1402 *	432	22	+ 1.3	0.04	1.5	1.3	120	4.7	20	3	5	3.5
MGF 1402 *	1296	18	+ 1.3	0.04	0.8	0.5	82	2.5	5	3	–	1

L_D: drain inductor
D_D: inductor internal diameter
l_D: length of L_D
n_D: numbers of turns of silvered wire 0.5 - 0.8 mm dia. for L_D

Table 2: Calculated of component values on the amplifier's characteristics. The following devices can be used in all amplifier versions without entailing component changes: MGF 1202, -1302, -1400, -1412, -1303, CFY 12, -13, -14.

The preamplifier housing is fabricated in accordance with **fig. 8** from 0.5 - 0.6 mm copper or brass sheet. The chip capacitors are soldered onto the screened wall on the same side as the screen is soldered to the box sides. This ensures that solder is kept from the vicinity of the helical resonator thus tending to keep losses low. The lower end of the coil L_1 is passed through a hole in the screen wall and then soldered. The trimmer capacitor C_t is a Johanson Air Tronic type 5200, 5270 or 5202. The coaxial connectors can be either "N" or BNC-types and are soldered on to the box. A degree of protection, as well as a stable supply voltage, is afforded by the three-terminal regulator 78L05.

6. A 432 MHz GaAs-FET PREAMPLIFIER

The circuit schematic of **fig. 9** indicates its close relationship with the 2-metre version. The output is also loaded with a resistance R_D in order that the amplifier is rendered unconditionally stable. A high-pass L-network, comprising a miniature disc or chip capacitor C_D and inductor L_D, matches the resistor/transistor to the 50 Ω output impedance.

In accordance with what has been discussed earlier, it is apparent that the optimal form of input circuit on this frequency is a coaxial resonator having a characteristic impedance of 77 Ω. Capacitive coupling is effected to the antenna. Fine tuning to resonance is carried out by a Tekelec or Johanson trimmer type 5200, 5202, 5700 or 5800 and the antenna coupling is made by a plate-capacitor fabricated in accordance with **figs. 10c and 10d**.

This type of trimmer ensures a minimum of circuit losses. Its dimensions and its distance to the resonator have been carefully dimensioned that the optimum calculated capacitance can be achieved in practice. This is important for the correct tuning of the amplifier for minimum noise as discussed earlier in the opening chapter.

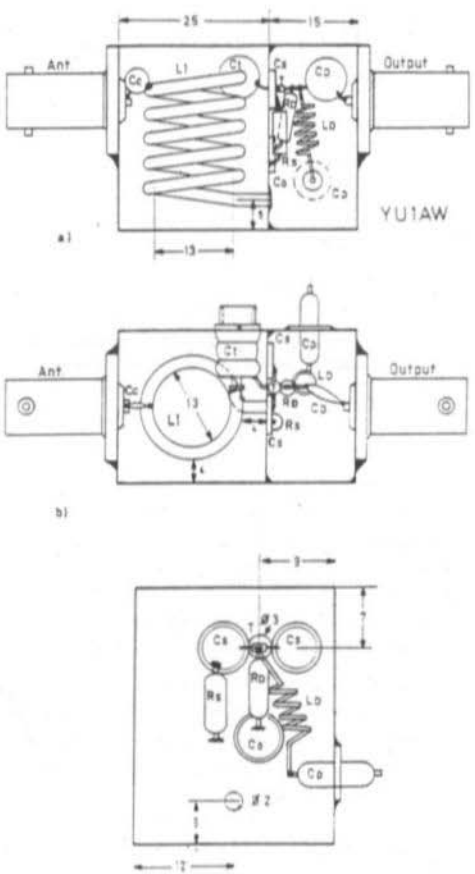

Fig. 7: Constructional details for the amplifier of fig. 6, a)side view, b) upper view, c) screen wall with mounted components

The drain current has to be adjusted to 10 to 15 mA (approx. 20 % of I_{DSS}) for each individual transistor. This is carried out by a process of changing the source resistance R_s until this current has been obtained. The source voltage U_{DS} will then be close to 3 V for FETs in the MGF-series, necessitating a value of 100 Ω for R_s, and 4 V for the CFY-series, R_s = 10 Ω.

The transistors MGF 1200, -1202, -1402, - 1400, -1412, -1302 and the CFY 12, -13 and -14, have

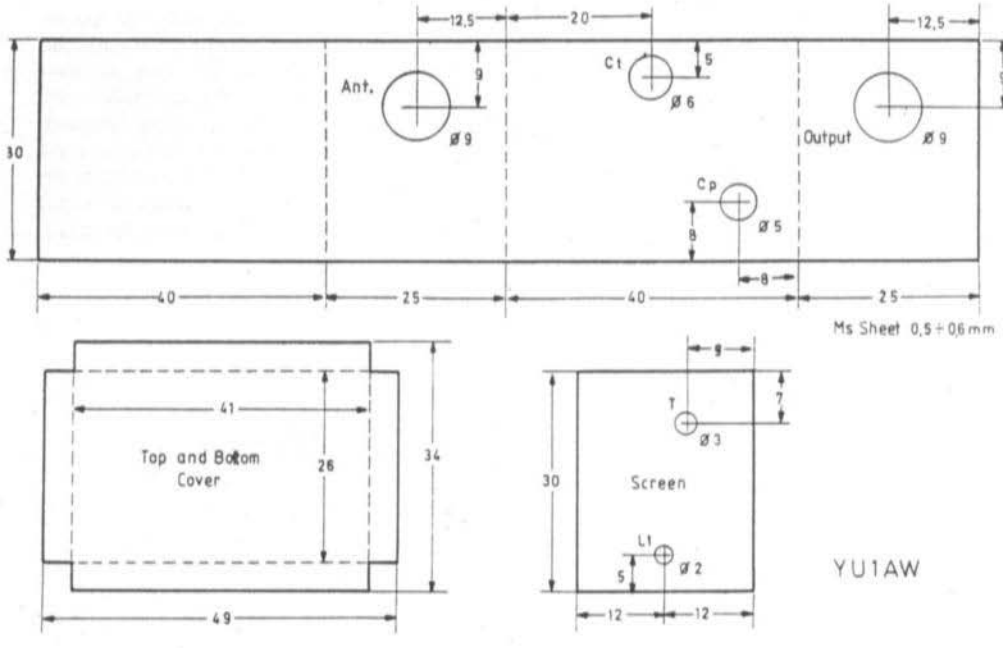

Fig. 8: Sheet brass parts for the amplifier of figs. 6 and 7

very similar S-parameters at this frequency and can be interchanged without any circuit alterations.

The housing, shown in **fig. 11**, is made from silvered brass sheeting 0.5 to 0.6 mm thick. It is fitted with a cover. The resonator is also silver-

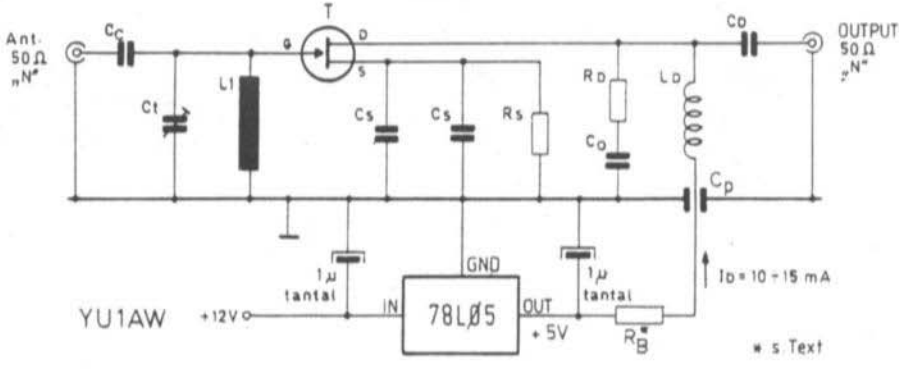

Fig. 9: Schematic of an unconditionally stable GaAs-FET preamplifier for 432 or 1296 MHz

coated and is fitted through a hole in the housing wall, protruding some 0.5 mm to the outside. It is then soldered to the wall. As by the 2-metre construction, there should be no solder in the interior of the coaxial resonator, this keeps losses low.

The capacitor C_c is also silvered brass plate from the same material as the housing. It is bent and fitted exactly 1 mm from the resonator and soldered. This is achieved conveniently by cutting a suitable piece of 1 mm cardboard and forming both cardboard and plate into the required shape. The combination is then pressed against the resonator and the plate soldered into position on the inner of the connector – the cardboard spacer is then, of course removed. Both the input and the output connectors are of the type N. The input socket is soldered to the case but it is probably better to fasten the output sockets with screws after assembling the output circuit.

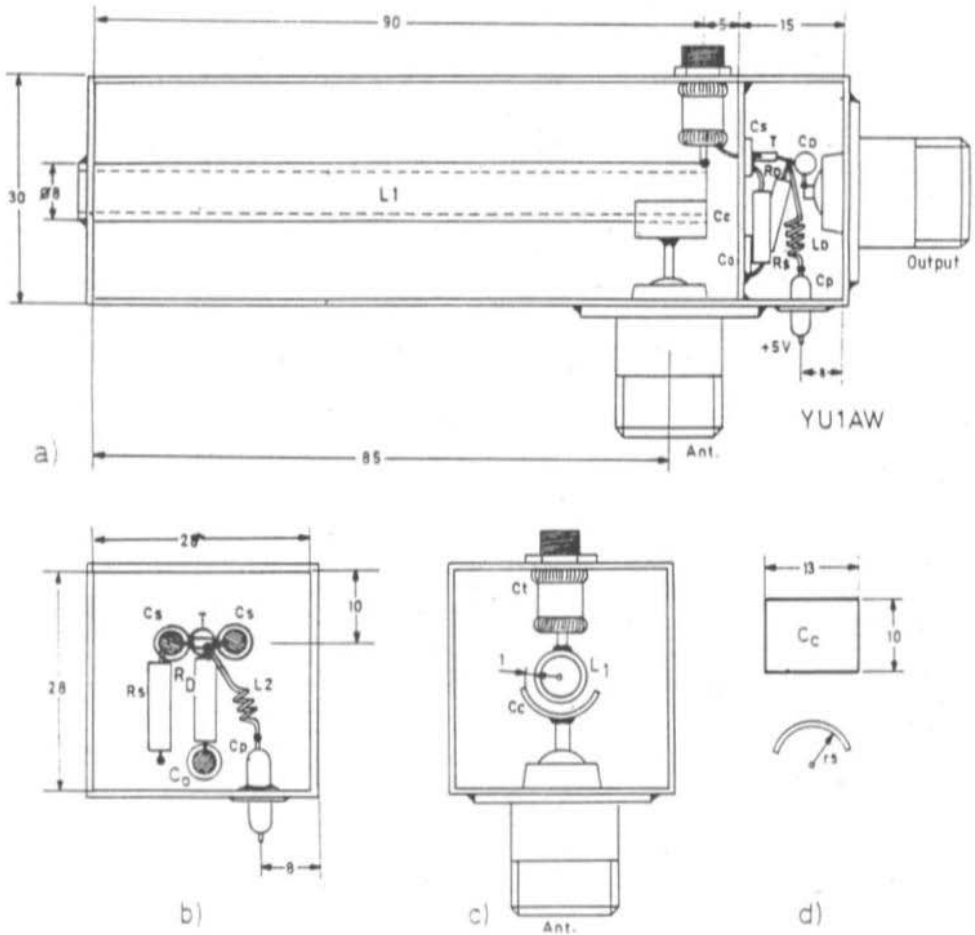

Fig. 10: Constructional details for the 432 MHz-version of the amplifier of fig. 9

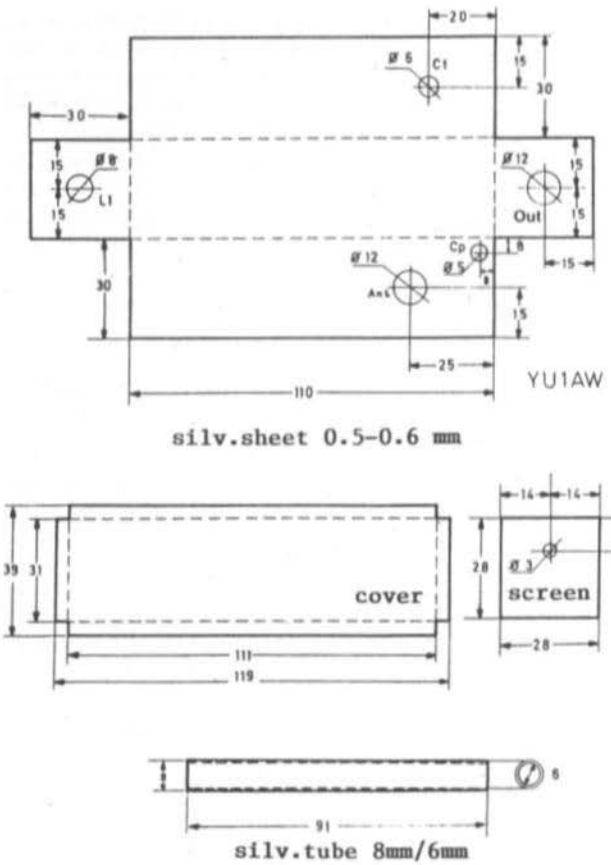

Fig. 11:
Dimensions for fig. 10

7.
GaAs-FET PREAMPLIFIER FOR THE 23 cm-BAND

As can be seen from **figs. 9 and 12**, only the size of the resonators differentiates the amplifiers for the 70 cm and the 23 cm bands. This also determines the overall size of the construction – the 23 cm unit being smaller.

Owing to the high frequencies particular care must be taken in the construction of the housing (**fig. 13**). The cover must be of a very good electrical fit all the way around its perimeter. The cover should be spot-soldered to the housing at a few equi-distant points around its edge after the assembly has been finished. Perhaps a better solution to this problem is that adopted by YU1IQ, who also constructed a version of this amplifier. This uses a box construction made from brass sheet (25 x 25 x 38 mm long) and is shown in **fig. 14**. The screening wall and the end walls are silver-soldered.

In order to circumvent the problem of the poor cover contact, two small windows were cut which were just large enough to permit the installation of the transistor, the plate capacitor C_c and the

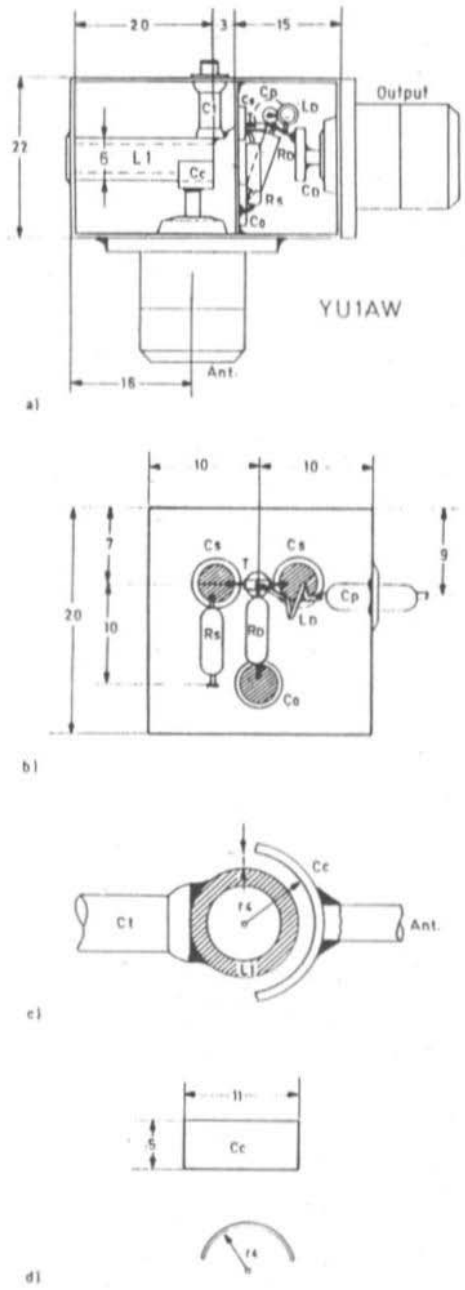

Fig. 12: Constructional details for the 1296 MHz-version of the preamplifier in fig. 9

other parts. The output circuit components can be assembled through the output connector hole. The windows can then be sealed by a cover using many small screws. The two sockets for input and output are also screwed on to the housing.

The silvered resonator has a 6.5 mm diameter and has a characteristic impedance of 77 Ω. It is provided with a 3 mm internal threaded end and is fastened to the housing with a good electrical contact by means of a suitable screw.

It is very important that at this frequency the highest grade of trimmer capacitor is employed for C_t. Suitable types are Tekelec and Johanson types 5700 or 5800 (0.3 - 3.5 pF). It is connected to the resonator by a screw-thread (see fig. 14).

The test measurements on both prototypes showed a very good conformity both with each other and with the theoretical predictions for amplification, noise-figure, input circuit loaded-Q and the output circuit matching. The unconditional nature of the stability was manifest under all input and output conditions. Also, the simple and precise tuning for minimum noise was carried out and then confirmed by measurement.

8. CONCLUSIONS

Even nowadays, many antenna preamplifiers designs are published and also manufactured without a consequent consideration of the problems concerning output matching and its wideband stability. The consequence is, that they are only conditionally stable over a limited range of frequencies and/or input and output impedances.

They appear to give satisfactory results thanks largely to the very low-noise factor of the active device employed. However, owing to poor design, the noise caused by input circuit losses often overshadows that from the transistor itself. The most agressively priced preamplifiers are among some of the worst cases in this respect. They are also adjusted to unnecessarily high gain (sells well!) making them unstable and problematical in operation.

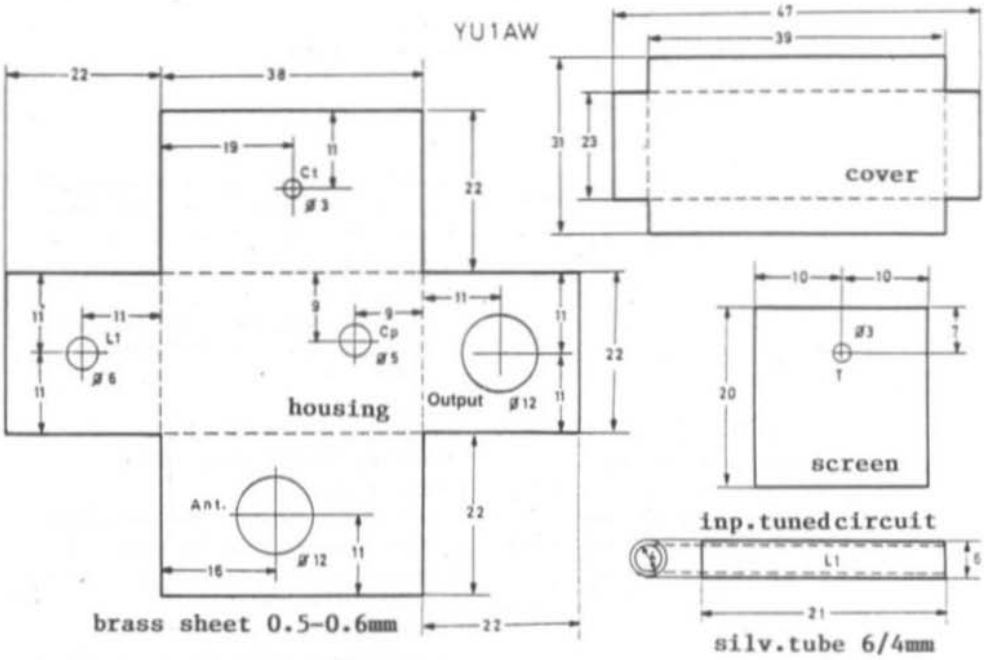

Fig. 13: Dimensions of the metal work for fig. 12

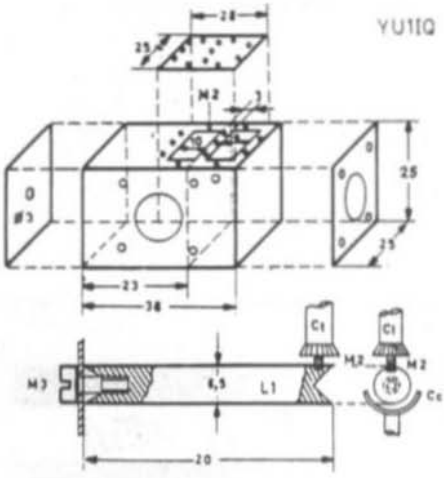

Fig. 14: YU1IQ's alternative version of the 1296 MHz-preamplifier based on a square-section tube of brass 25 x 25 mm

In order to make a valid evaluation of the performance of a preamplifier, the following criteria are offered:–

* The input circuit transformation must be adjusted for minimum noise and not for maximum overall gain.
* The input circuit must have a minimum of losses in order to keep the noise due to these losses from exceeding that produced by the active device itself.
* Over a wide range of frequencies and also input/output impedances, the amplifier must show no signs of instability.
* Output matching to the following stage must be good (low VSWR) thus providing it with a good source impedance.
* Posses just sufficient gain to minimize the second-stage noise contribution to the overall noise figure.

The application of these criteria to the preamplifiers described in this article have the following consequences:

1. A fixed capacitor C_c enables the input to be precisely and easily tuned to the minimum noise condition.
2. A careful calculation of the optimum values for the input circuit elements for minimum loaded-Q, choice of resonator type for the maximum possible Q_u and the use of high-Q trimmers all ensure a minimum of circuit loss.
3. The calculation of the exact loading of the device's output circuit to achieve an unconditional stability factor i.e. $K > 1$.
4. The above drain-circuit evaluations entail repeated calculations of the S-parameters of the device plus resistor, then output matching for maximum gain. This ensures an unconditionally stable amplifier with a low output VSWR together with a high gain.
5. The gain degradation resulting from the loading of the device by the drain resistor R_D should only result in the loss of a few dBs but this loss is easily accommodated by the very high gain exhibited by GaAs-FETs at these low frequencies. The overall gain available is usually in the region of 20 dB – more than enough for all practical applications.

9. REFERENCES

(1) Dobričić, D., YU 1 AW: Low-Noise 144 MHz Pre-Amplifier using Helical Tuned Circuits VHF COMMUNICATIONS, Vol. 19, Ed. 4/1987, P. 243 - 252

(2) Nollis, W.C.: Design of Transmission Line Tank Circuits Electronics Manual for Radio Engineers, 1949, P. 748 - 752

(3) Motorola AN-421: Semiconductor Noise Figure Considerations Motorola RF-Data Manual 1980

(4) Vatt, G., KB 0 O: Computer-aided UHF Preamplifier Design Ham-Radio Magazine, Oct. 1982, P. 28 - 35

(5) Froehner, W.H.: Quick Amplifier Design with Scattering Parameters Electronics, Oct. 1967, P. 5 - 2 to 5 - 11

(6) Bertelsmeier, R., DJ 9 BV: How to achieve a low system temperature on 432 MHz EME Paper prepared to the 3rd Intern. EME Conference in Thorn/Nederlands, Sept. 1988

(7) Molitor, L., W 7 IUV: Taming a Preamp 2 Metre EME Bulletin, No. 45, Dec. 1987

Matjaž Vidmar, YT 3 MV

Amateur-Radio Applications of the Fast Fourier Transform Part 2b (Concluding)

5. AMATEUR APPLICATIONS OF A FFT SPECTRUM ANALYZER

Although FFT spectrum analysis is presently limited to the audio-frequency range or slightly above, it has many interesting and very useful amateur-radio applications. In the following section a few typical amateur-radio applications will be presented including the spectrum plots and intensity spectrograms obtained. All of the latter were obtained by connecting the output of an amateur SSB or FM receiver to the MC68010 based DSP computer described in a series of articles in UKW-BERICHTE/VHF COMMUNICATIONS. All of the plots were obtained with a FFT spectrum analyzer program including a 1024-point FFT algorithm and all the other features described in the previous section. Unfortunately the intensity spectrograms could only be printed in black-and-white with no grey levels, so they can not represent all of the information that was visible on the computer screen.

A FFT spectrum analyzer is a useful tool when building a SSB receiver or transceiver. One of the most difficult tasks when building a SSB receiver is to measure the passband of the crystal filters used, regardless whether are they homebrew or commercially available items. To obtain a reliable result, a very stable sweep generator is required in addition to a storage oscilloscope due to the slow sweeping speed required. Alternatively, a FFT spectrum analyzer can be connected to the receiver audio output and a wideband noise source to the receiver input (if the receiver own noise is not sufficient). Thanks to the speed of the FFT spectrum analysis the result can be obtained quicker than with the sweep generator, allowing real-time tuning of the trimmers in and around the crystal filters. Two typical results, plotted on a logarithmic amplitude scale, are shown on **fig. 5.1.**: a 2 kHz SSB filter above and a 500 Hz CW filter below. Using FFT spectrum analysis, the tradeoff between accuracy and speed is selected by choosing the averaging factor. However, even with no averaging, the FFT analysis will only provide a noisy plot while a too fast sweep generator will provide a completely distorted and thus useless result.

A FFT spectrum analyzer is able to reliably detect very weak signals hidden in noise, far beyond what a human ear can do, since it is not limited to certain frequency bands, resolution

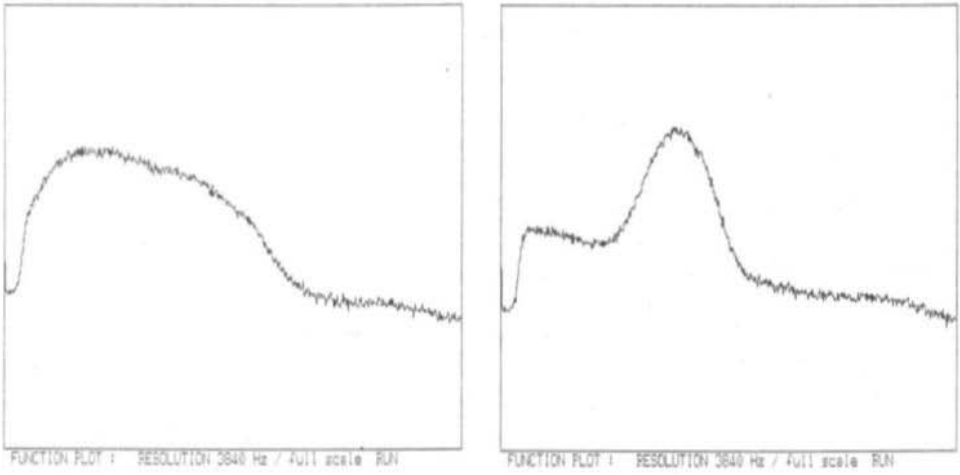

Fig. 5.1.: Audio frequency response of a SSB receiver: left with SSB filter, right with CW filter

bandwidths or averaging intervals. The plots on **fig. 5.2.** were obtained by tuning a 2 m amateur SSB receiver to a weak CW beacon and then decreasing the signal level with an input attenuator to obtain a signal-to-noise ratio of about −15 dB in a 2.5 kHz bandwidth or −5 dB in a 250 Hz bandwidth. Although the signal-to-noise ratio is around +10 dB in the spectrum analyzer resolution bandwidth, some averaging is required to reliably detect the signal. On the frequency/amplitude plot (above on fig. 5.2.) the averaging was performed by the computer and then the

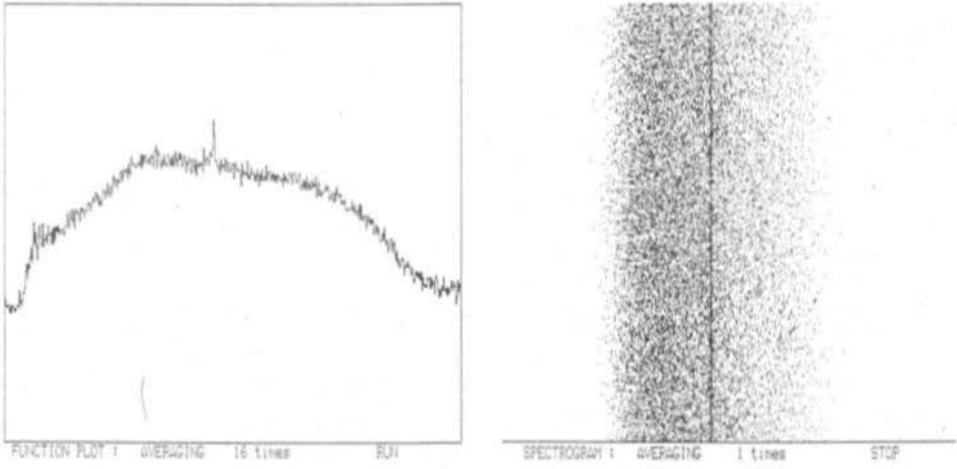

Fig. 5.2.: Weak signal detection: averaging, LOG scale (left) versus intensity spectrogram (right)

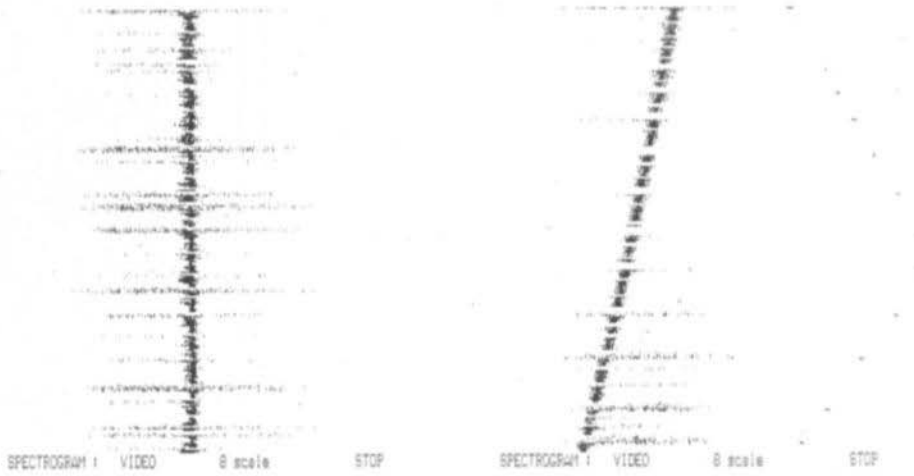

Fig. 5.3.: CW signal with a slight "FM-ing" (left) and affected by a quickly changing Doppler shift (right)

result was plotted. On the intensity spectrogram (below on fig. 5.2.) no averaging was performed by the computer. Averaging is, however, performed by our eyes when observing the spectrogram!

Even weaker signals could be detected either by increasing the frequency resolution or by increasind the averaging factor or both. The practical limit is mainly imposed by the time required for the signal to be available for a reliable detection. In a practical communications system there are other constraints too: receiver and transmitter frequency instability or phase noise and propagation effects. The FFT spectrum analyzer can solve the problem of frequency uncertainty, since it allows to observe a frequency band of a few kHz instantaneously with a resolution of 5 to 10 Hz. The phase noise of transmitters and receivers should be minimized anyway. Unfortunately, some propagation effects also show up as phase or amplitude noise, especially in EME (moonbounce) communications. These effects are proportional to the carrier frequency so major advantages of using FFT techniques for EME communications can only be expected on VHF and UHF frequencies. On these frequency bands FFT signal processing may decrease the RF link performance requirements by 10 to 20 dB, since higher figures would result in useless data rates. In any case, a communications protocol has to be agreed upon before these techniques can be used: hand-keyed CW is certainly not a good choice for computer processing.

Fig. 5.3. shows how a Morse-keyed CW transmission looks on an intensity spectrogram. The keying was too quick for the dots and dashes to appear on the spectrogram, the interruptions correspond to the longer spaces between letters. In order to be able to see the single dots, much more frequent FFTs should be made and each FFT should be taken on less data samples since time and frequency resolution are of course reciprocal.

Receiver AGC effects are easily visible, increasing the noise level during longer pauses. The spectrogram above was obtained from the AO-13 Mode-B 2 m beacon and shows a slight "FM-ing": the trace has "tails" to the right at the beginning of each transmission. The spectrogram below was obtained from the LUSAT-1 70 cm CW beacon. A quickly changing Doppler frequency shift is easily visible, as well as an interference to the left corresponding to the third harmonic

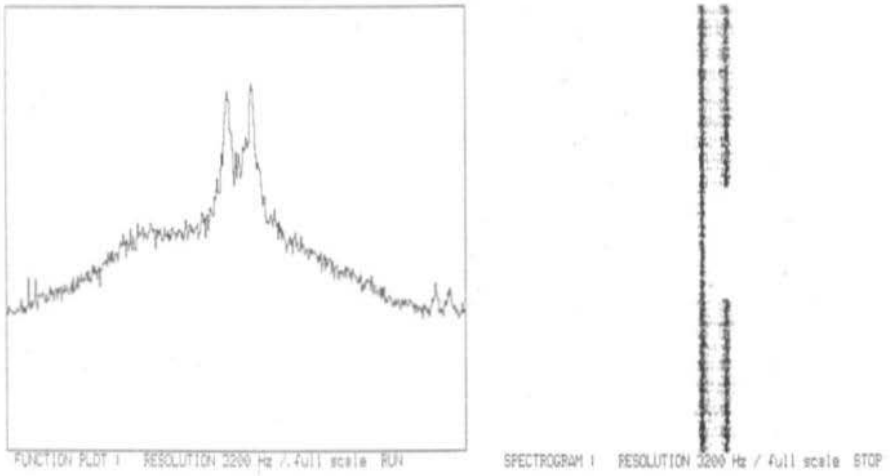

Fig. 5.4.: FSK RTTY signal spectrum: LOG vertical scale (left) and intensity spectrogram (right)

of the signal, generated somewhere in the audio stages of the SSB receiver.

A FFT spectrum analyzer can be used to identify, tune-in and measure the parameters of a FSK RTTY transmission as shown on **fig. 5.4.** The two RTTY tones are easily visible both on the amplitude/frequency display and on the intensity spectrogram. Both of them were obtained from the AO-13 50 baud RTTY Mode-B beacon. In the middle of the spectrogram a period with no keying is visible: only one of the tones, unmodulated, is transmitted during this period. During

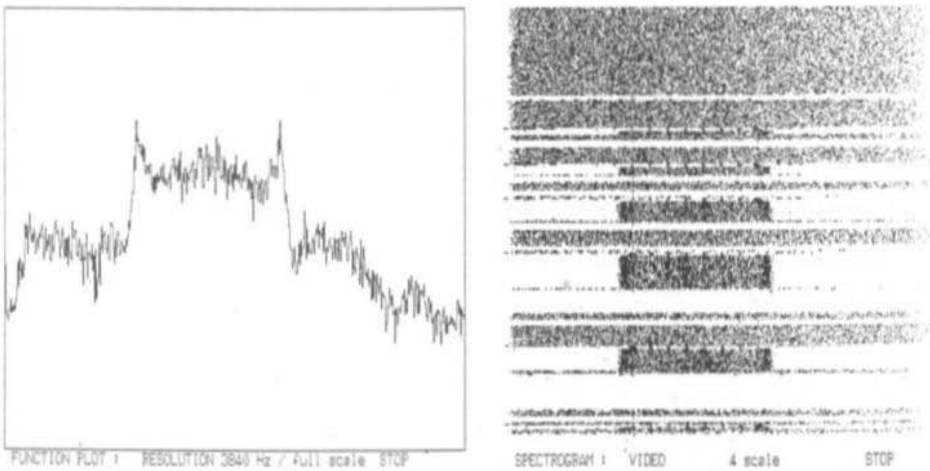

Fig. 5.5.: AFSK 1200 bps packet-radio signal spectrum: LOG vertical scale (left) and spectrogram (right)

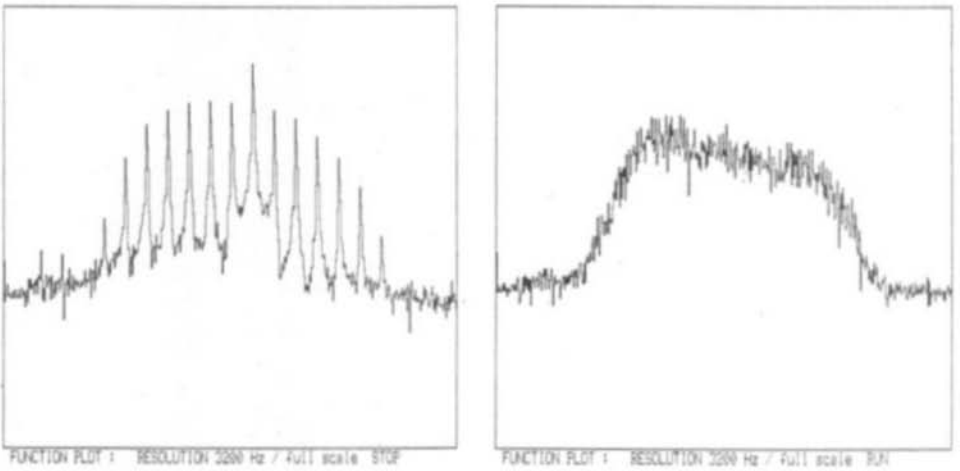

Fig. 5.6.: 1200 bps satellite PSK packet-radio transmission: flags (left) and data (right)

active keying the tone traces become wider due to the 50 bps modulation sidebands.

A FFT spectrum analyzer can therefore be considered as an up-to-date replacement for the oldfashioned RTTY oscilloscope tuning indicator. Both tone frequencies and the keying shift can be quickly and accurately determined. In addition, a FFT display provides information about signal distortion (selective fading) or interferences. Especially in the latter case a FFT display will provide some useful information about the countermeasures to be taken (notch filter tuning for example) and about their effectiveness.

The parameters of a FSK or AFSK signal are more difficult to identify if the data rate is comparable to the frequency shift, as shown on **fig. 5.5.** 1200 bps packet-radio uses 1200 Hz and 2200 Hz tones, the shift is therefore 1000 Hz, comparable to the data rate of 1200 bps. The spectrum of such a transmission is an almost contiguous frequency band with just a few peaks, that do not necessarily correspond to the tone frequencies as shown on fig. 5.5. above. The intensity spectrogram below shows the intermittent nature of packet-radio signals. Due to the short duration of the packets, their spectrum could never be obtained by a scanning-receiver type spectrum analyzer.

A FFT spectrum analyzer can be used as a valuable tuning aid for PSK packet-radio communications. Phase-shift keying is used for satellite packet-radio communications since it allows a longer communications range with the same RF equipment performance. On the other hand, PSK and other coherent techniques require accurate tuning and good frequency stability.

The spectrum of a 1200 bps packet-radio transmission from the PACSAT-1 satellite is shown on **fig. 5.6.** The plot above shows the spectrum during the transmission of flags between the packets. On this plot it is easy to identify the carrier, surrounded by sidebands spaced at 150 Hz. During the transmission of packets containing random data the spectrum looks almost like perfect noise (fig. 5.6. below) and it is much more difficult to identify the correct tuning. In fact a straightforward PSK transmission contains very little redundancy and there are no residual carriers either.

Some more redundancy can be noticed in the AO-13 400 bps BPSK Mode-B beacon transmission due to manchester coding. **Fig. 5.7.** above shows the spectrum during the transmission of the filling bytes (50 H) in between the data frames: this repetitive pattern generates

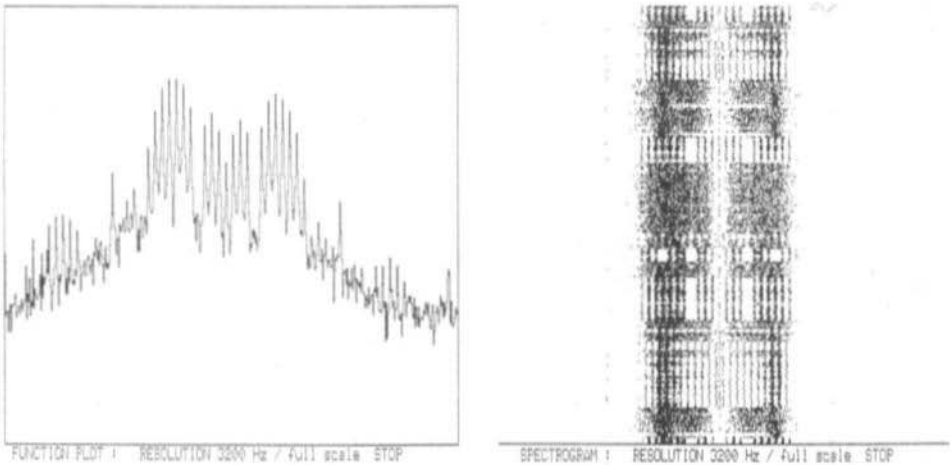

Fig. 5.7.: AO-13 400 bps BPSK telemetry spectrum: LOG vertical scale (left) and intensity spectrogram (right)

the many discrete spectral lines. On the intensity spectrogram on fig. 5.7. below it is easy to identify the single data frames and the filling byte periods in-between them. Even data frames sometimes contain repetitive patterns causing discrete spectral lines inside the data frames. Regardless of the modulation data the signal spectrum has two main lobes caused by the manchester coding. The latter are positioned symmetrically around the carrier, suppressed by this modulation technique.

A FFT audio spectrum analyzer is useful to check WEFAX and APT satellite signals and related receiving equipment. Using a FFT spectrum analyzer important details of an unknown satellite transmission, like that of a new satellite, can easily be determined. Further, the receiving equipment can be checked for a correct de-emphasis (to avoid loosing geometrical resolution) and sources of eventual interferences.

All this is easier to describe on a well known example, like the Meteosat WEFAX transmission shown on **fig. 5.8.** On the frequency/amplitude plot on fig. 5.8. above the strongest spectral component is the 2400 Hz subcarrier. The subcarrier should be surrounded by symmetrical sidebands if the deemphasis is properly adjusted. The sidebands depend of course on the picture content. The most notable detail are the two symmetrical peaks corresponding to the line-sync 840 Hz bursts. These have a rather rounded peak, since their duration is very short: their spectral width is inversely proportional to their duration. The intensity spectrogram shown on fig. 5.8. below shows that the sync bursts appear in about every second FFT conversion. Also, the spectrum close to the 2400 Hz subcarrier also changes with the picture line period. The annotation transmitted at the end of the picture is well visible, followed by the discrete spectral lines of the 450 Hz stop tone lasting 5 seconds. What follows is just part of the spectrum of a DCP retransmission between two WEFAX pictures. The DCP flags create two strong discrete spectral line traces on the spectrogram, interleaved with three DCP data frames visible on fig. 5.8. below.

The spectrum of a NOAA APT transmission, shown on **fig. 5.9.** is a little more complex. There still a strong 2400 Hz subcarrier component, but there are two different sync bursts of 832 Hz and 1040 Hz respectively. The sidelobes generated

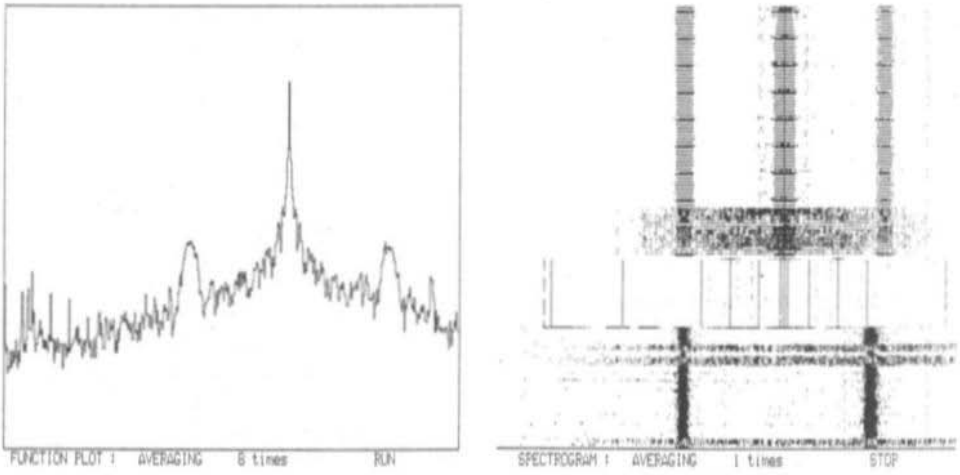

Fig. 5.8.: METEOSAT WEFAX signal spectrum: LOG vertical scale (left) and intensity spectrogram (right)

by both sync bursts are well visible on fig. 5.9. above. On the intensity spectrogram on fig. 5.9. below it is easy to notice that these sync pulses appear interleaved in the APT signal. The remaining spectrum also changes with the same period.

Although a FFT spectrum analyzer is actually an audio-frequency test equipment, it has many interesting applications in the amateur-radio field. The above examples were chosen just to show a few possible applications of a FFT spectrum analyzer and the many different ways a

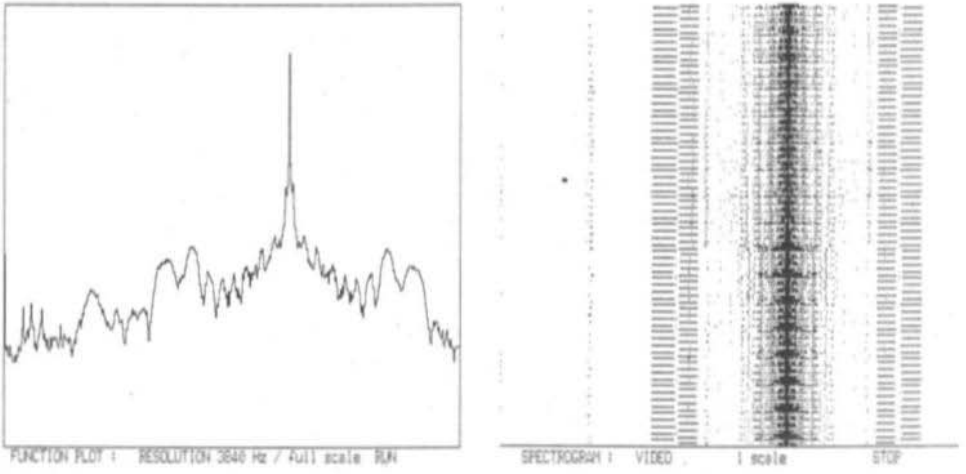

Fig. 5.9.: NOAA-10 APT signal spectrum: LOG vertical scale (left) and intensity spectrogram (right)

FFT spectrum analyzer can be used. Probably most of the applications are yet to be discovered, since FFT spectrum analysis only became available to amateurs with recently developed low cost and high performance microprocessors and A/D converters.

6. THE FFT SPECTRUM-ANALYZER PROGRAM FOR THE DSP COMPUTER

The FFT algorithm can be implemented on almost any digital computer, ranging from 8-bit video-game toys to the largest and fastest mainframes. The FFT algorithm requires very little memory, since the results of a "butterfly" operation are stored in the same two memory locations where the arguments were taken from. Therefore the memory requirements are very low, including just a buffer of the size of the input data block and another buffer of a similar size to hold the phase coefficients.

Of course the execution time will depend on the computer used. Computing a 1024-point complex FFT on a 8-bit microcomputer programmed in a high-level language like BASIC will require several minutes. Computing the same 1024-point FFT on an IBM AT compatible equipped with the mathematical coprocessor and executing a compiled program will still require several seconds. A well-written machine code program for a general-purpose 16-bit microprocessor can compute a 1024-point FFT in a few hundred milliseconds using 16-bit integer arithmetics. Finally, dedicated DSP microprocessors are able to compute a 1024-point FFT in tens of milliseconds with the top-of-line devices requiring a few milliseconds.

A FFT spectrum-analyzer program was written for the DSP computer published in UKW-BERICHTE/VHF-COMMUNICATIONS. This computer includes a 8-bit logarithmic A/D converter input port and a 512-pixel by 256-line, 256-grey-level video display. The MC68010 microprocessor used in this computer is able to compute a 1024-point complex FFT in about 150 milliseconds. Considering that some CPU time is required for other functions too, like interrupt handling or display update, the maximum sampling frequency for successive but non-overlapping FFTs without skipping any input data is about 8 kHz. This figure matches very well the performance of the switched-capacitor filter in front of the A/D converter as well as the audio bandwidth available from a communications or amateur receiver.

The FFT spectrum-analyzer program for the DSP computer includes all of the features from fig. 4.1.: A/D conversion, data buffering, FFT algorithm with magnitude computation and display. Weighting, averaging, LIN/LOG conversion, display format and hardcopy are implemented as user-selectable options. The complete set of commands is shown on **fig. 6.1.** The same HELP menu is obtained each time a wrong command is issued. Otherwise, the program uses 248 image lines for the function plot or spectrogram and the 8 bottom lines to annotate the main program parameters.

The program parameters are selected by typing their initial letter as shown on the HELP menu. The selected parameter will then appear in the annotation text line. The selected parameter value can be then adjusted: increased or decreased, by using respectively the + and – keys. The * key will set ALL of the parameters to their default values.

The program parameters include:

AVERAGING: averaging factor, ranging from 1 (no averaging) to 4096 and adjustable in powers of 2.

BORDER, DIVISIONS, ERASER, INK, PAPER: grey-level count, adjustable between 0 and 248 in steps of 8.

FUNCTION DISPLAY: selects an amplitude/frequency function-plot type display as indicated in the annotation text.

```
*** IMPLEMENTED COMMANDS ***

  +    Increment parameter
  -    Decrement parameter

  A    Averaging: factor
  B    Border: grey-level
  D    Divisions: grey-level
  E    Eraser: grey-level
  F    Function display
  G    Gain: A/D converter
  H    Hardcopy: create file
  I    Ink: grey-level
  O    Overlap: ON / OFF
  P    Paper: grey-level
  R    Resolution: full scale
  S    Spectrogram display
  T    Trigger: RUN & STOP
  V    Video: gain steps
  W    Weighting: raised-cosine ON / OFF

  X    Set default parameters

  FF   Clear screen & Update border, divisions, paper

  CR   Exit

*** Press any key to exit!
```

Fig. 6.1.: Help menu of the FFT spectrum-analyser program showing all implemented commands

GAIN: adjusts the gain between the A/D converter output and FFT input to increase the dynamic range with low-level signals. Usually set to 1 to prevent saturation.

HARDCOPY: each time H is depressed, a hard-copy file PLOT.DAT is created. The format is selected to be understood by most dot-matrix and laser printers. Since these printers can not print grey levels, the treshold between black and white is set to a grey-level count of 127/128!

OVERLAP: switches the overlap (50 %) option ON or OFF (toggle operation). When ON, the overlap option is indicated by an "O" in the annotation text.

RESOLUTION: selects the sampling frequency and therefore the full-scale frequency span or resolution between 301 and 6400 Hz by setting the sampling-frequency divider modulo.

SPECTROGRAM DISPLAY: selects an intensity spectrogram type display, as indicated in the annotation text.

TRIGGER: starts or stops (toggle operation) the operation of the spectrum analyzer. The status RUN or STOP is indicated in the annotation text. In the STOP mode, the display is "frozen".

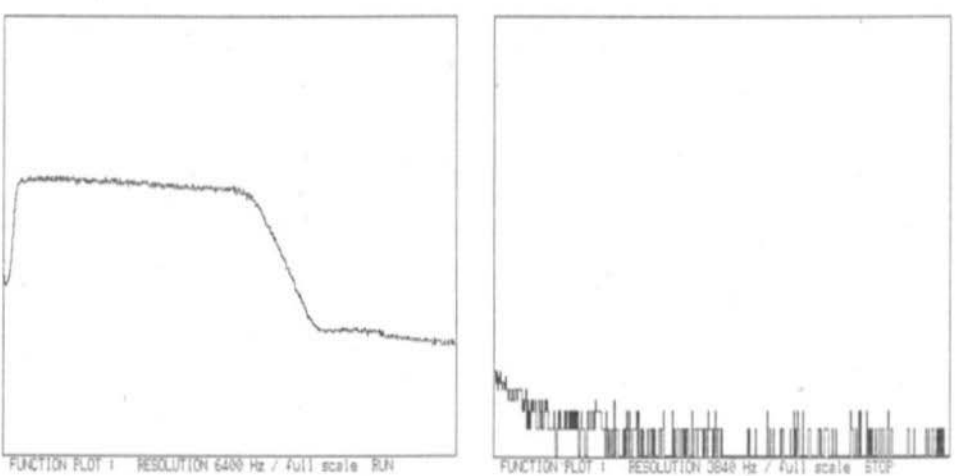

Fig. 6.2.: TP 3040 input filter passband (left) and MK 5156 A/D converter noise with no input signal (right)

VIDEO: selects the video gain after the FFT algorithm in the LIN mode. The lowest setting selects a LOG video scale (default).

WEIGHTING: switches the raised-cosine weighting option ON or OFF (toggle operation). When ON, the weighting option is indicated by a "W" in the annotation text.

The performance of this FFT spectrum analyzer is of course limited by the analog hardware used: input bandpass filter and A/D converter. **Fig. 6.2.** above shows the passband of the input filter, obtained with the same spectrum analyzer by simply connecting a wideband noise source to the input. The dynamic range of the 8-bit logarithmic A/D converter used is only about 40 dB due to quantisation noise. The performance of the spectrum analyzer is however better: in many practical cases the display dynamic range reaches 60 dB since the quantisation noise usually appears as wideband noise.

The input switched-capacitor filter and A/D converter own noise is well visible on fig. 6.2. below. Using a logarithmic amplitude display the quantisation steps become very large at low signal levels. In the LOG vertical mode, the full scale amplitude range is 15 bits or 90 dB. The difference between counts 1 and 2 should therefore correspond to the difference between counts 16384 and 32768 on a LOG scale, however in the former case there are no additional counts possible between 1 and 2 resulting in relatively large "steps" on the display.

With a 10 MHz CPU clock, the FFT spectrum-analyzer program is able to operate with a sampling frequency of about 8 kHz (resolution 4 kHz) on contiguous but non-overlapping data. The input data buffer routine is designed to skip data blocks automatically if the CPU is unable to further process them in real time, like in the case of a higher sampling frequency or overlapping FFTs. Sometimes it is very useful to be able to operate in these conditions even if some data is lost. On the other hand, an analog scanning-receiver type spectrum analyzer usually discards over 99 % of the information contained in the input signal!

The FFT program includes a 1024-point complex FFT algorithm. The algorithm is used to process two independent sets of 1024 consecutive input samples. The results of the FFT are then separated using the Fourier transform symmetry laws into two independent 512-point signal spectra. The phase information is rejected and the magnitudes are computed using a quick approximation for the square root. The LIN/LOG conversion is obtained with a lookup-table algorithm to avoid the even slower log function.

The display routine includes automatic limiting if the magnitude exceeds the top on a function plot or the maximum brightness on an intensity spectrogram. Hardcopies of the computer screen in the various modes are used throughout this article.

The FFT spectrum-analyzer program is written partially in the MC68010 machine code and partially in the DSP computer high-level language. The commented source program is about 15 kilobytes long while the compiled program requires about 47 kilobytes. This is actually less than most other DSP programs thanks to the compactness and low memory requirements of the FFT algorithm. Of course the FFT program can run in multitask with other programs that do not use the same peripherals, like the TRACK program.

Future upgrades to the FFT spectrum-analyzer program should include the capability to adjust the size of the FFT (number of points) according to the requirements of the measurement: some problems (quickly changing signals) require less than 1024 points while others require a higher resolution and thus more than 1024 points. The 1024-point FFT is however a good compromise for most measurements.

Finally, it is hoped that this article will encourage amateurs to use the FFT algorithm and FFT spectrum analysis, since the latter can easily be implemented on the described DSP computer and on many other computers as well. Presently FFT spectrum analysis is only available on top-of-line professional instrumentation and the reason for this is probably the poor understanding of this new technique by the majority of spectrum-analyzer users.

7. LITERATURE

(1) Vidmar, M., YT 3 MV:
Digital Signal Processing Techniques for Radio Amateurs
Theoretical Part
VHF COMMUNICATIONS Vol. 20, Ed. 2/1988, P. 76 - 97

Part 2: Design of a DSP Computer for Radio Amateur Applications
VHF COMMUNICATIONS Vol. 21, Ed. 1/1989, P. 2 - 24

Part 3: Construction and Use of the DSP Computer
VHF COMMUNICATIONS Vol. 21, Ed. 2/1989, P. 74 - 94

Part 4a: Application Software
VHF COMMUNICATIONS Vol. 21, Ed. 3/1989, P. 130 - 137

Part 4b: Application Software
VHF COMMUNICATIONS Vol. 21, Ed. 4/1989, P. 216 - 227

Amateur-Radio Applications of the Fast Fourier Transform – Part 2a
VHF COMMUNICATIONS Vol. 22, Ed. 3/1990, P. 130 - 138

Detlef Burchard, Box 14426, Nairobi, Kenya

A Short-Wave Receiver PLL

The present boom in radio pagers, radio telephones and cellular radio has led to the development of the PLL integrated circuit. The high frequencies involved in these activities have necessitated newer techniques namely, the sample-hold detector which, together with a frequency/phase detector incorporated into a single IC package, is beginning to represent the latest state of the art in this technology. These techniques could, however, be obtained from Valvo (Philips) as standard CMOS ICs some 10 years ago. This fact is what this article is about. Obtaining the IC is simple, every mainline electronic supplier has them in stock. The BCD-orientated frequency input is particularly interesting from the single-project point of view.

The mass-production items mentioned above are usually accompanied by processor control or a system control memory. The binary frequency input is then, only advantageous because storage capacity can be saved. The PLL IC involved, Plessey NJ8820, Philips TDD1742T, Siemens TBB200 etc., require only the addition of a PROM for it to be used. The development has gone a little further. Philips announced the UMA1010T IC in 1989 which also contained an in-built prescaler usable up to 1150 MHz together with an op-amp. Other firms will follow suit.

The designers are hereby challenged! Who will bring out, after Borchert (Funkschau 13/89 and VHF COMMUNICATIONS 2 + 3/90) the first single-chip PLL? As the integration of the PROM is the next logical step. Let's hope that the consumer boom in HF mass production consumer goods is maintained!

1. INTRODUCTION

The ability of a shortwave receiver to be simply and accurately tuned to the desired sender frequency, is of the utmost importance for the instrument's acceptance by the user. The normal listener isn't interested in studying manuals on how to tune the receiver before he is able to get

the desired foreign station but receiver development has, unfortunately, tended to run in this direction. Ways in which a shortwave receiver could be developed to enable it to be operated by Granny have been published in (3). Digital tuning is the most logical development. Because of the frequent changes of wave-length necessitated by diurnal conditions, changes in sender location, sunspot activity etc., the received frequency must be readily programmable from the information held in schedules and frequency tables. More should and may not be necessary in order to tune the receiver to give the best possible reproduction under the prevailing propagation conditions.

Whether the desired frequency input is presented to the receiver by means of a selector switch, a keyboard or a computer is of no account as far as the local oscillator is concerned. The end effect is, that a digital word has been translated into the desired frequency and the prerequisite for this is the phase-locked loop. The nominal frequency is selected by BCD input switches which also serve both as the frequency indicator and the long-term memory. The inclusion of a built-in computer and other complex tuning is, of course, possible but is not the object of this article. The requisite conditions for the dimensioning of the PLL for this purpose will, however, be considered. Other applications may be derived from them.

2. THE OBJECTIVES

From the concept outlined in (3), the receiver IF will lie at the high frequency of 40.000 MHz and the receiver input tuning range will be from 4 to 28 MHz. The local oscillator (LO) will then have to cover the range 44 MHz to 68 MHz in one continuous tuning sweep. The basic frequency resolution should be 1 kHz, requiring a 5 decimal place, nominal-frequency input. Interpolation within ± 1 kHz may well be desirable for some purposes (SSB) and may be realized easily by increasing the resolution by a further two decimal places down to 10 Hz.

The PLL must take account of the IF offset and also provided with means to access facilities other than the normal IF.

The design should enable the digital word containing the received frequency to be taken from a memory or a computer. The latter could also be used to check the quality of the received signal according to pre-set criteria and automatically switch to an alternative frequency should this become necessary.

The PLL should be constructed of common proprietary ICs which are chosen to optimally fulfil the design objectives. Price considerations should play no part in the choice of components but naturally the costs cannot be allowed to rise out of all proportion.

3. WHAT SORT OF FREQUENCY DETECTOR?

The task of the loop detector is to lock the nominal frequency to that of the reference frequency. The choice of integrated frequency detectors is not extensive – there's actually only one type available! This is an arrangement of JK flipflops which first appeared in the MC4044 chip some 20 years ago. It has the useful characteristic of detecting large frequency dispositions with the correct change polarity. At frequency parity with the reference frequency it automatically becomes a phase detector and at phase parity (theoretically) it delivers no spurious voltages at its output. This arrangement will be referred to here as a frequency/phase detector (FP type).

All the other arrangements which are obtainable in chip form and can fulfill the required conditions, are primarily pure phase detectors. If they are used in a frequency controlled loop, care must be taken that the frequency is captured within the confines of ± 90° - 180°. The usual method to ensure this is by judicious output filtering in order that the VCO is periodically swept through the frequency range of interest. Better still is the combination with the correct type of

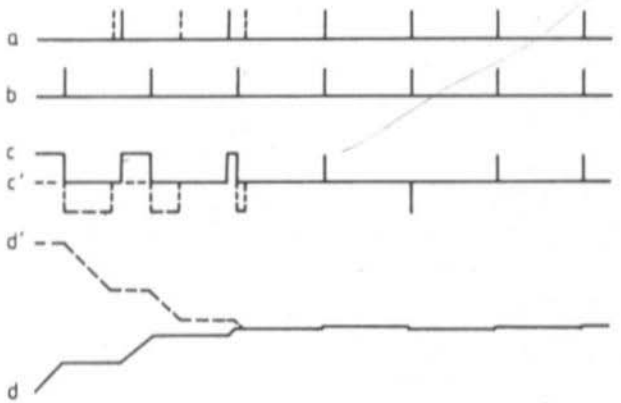

Fig. 1:
Signal waveforms in a frequency phase detector
a nominal pulse train
b reference pulse train
c quasi-state output
d integrator output at falling frequency

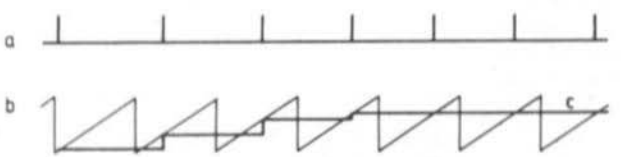

Fig. 2:
Signal waveforms in a Sample-Hold phase detector
a nominal pulse train
b reference pulse train
c output voltage

frequency detector. There are three types of frequency detectors, in integrated form, which are of interest: the EXOR type, the RS FF type and the SH type. The first two, when they are aligned, deliver a spurious output from the reference frequency; the third type is free from this defect. This latter type is the sample-hold (SH) and is the most familiar of this class of detector. Its use in automatic controllers has been dealt with in (2) but this was by no means the first description of a chopper-bar controller.

In (3), the sideband noise of the local oscillator was measured, and found to be suitably low. A frequency control loop should not introduce additional noise into the system. This means, in effect, that the frequency control (tuning) voltage should have no superimposed AC components on it when the loop is in the lock condition. Actually, the sideband noise of the system should be expected to improve by the use of the control loop. How far that can be true will be examined later on.

The residual components of the reference frequency can, of course, be filtered-out of the tuning voltage. Most books dealing with the subject do not fail to mention the consequence of this, namely the delay in achieving lock. It is a better practice to prevent the spurious signals from contaminating the control voltage in the first place. The other two members of the list of three, the FP and the SH types, will now be examined a little closer.

Fig. 1 depicts the process by which the FP type achieves the locked condition. The solid line indicates a rising nominal frequency and the broken line is that of a falling nominal frequency. The circuit has an in-between (quasi) state output c which fluctuates between V_{DD} and open circuit as long as the nominal frequency a is below the reference frequency b. In the reverse case, it switches between V_{SS} and open. In the ideal case, the circuit, when in the locked condition, would deliver no pulses at its output c. That, however, is not a stable condition. The VCO does drift off the nominal frequency from time to time and a pulse then appears. This pulse has a definite minimum duration which is determined by the internal characteristics of the IC. The

nominal frequency is supplied in the form of rectangular pulses and the IC must first of all produce needle pulses representing a signal flank which will be used to control the JK flipflops. This takes place under the control of gating pulses which are determined by the speed of the logic family under consideration. The IC is able to function even under the most unfavourable circumstances as the needle pulse widths will always be greater than the rise times of the flipflops, 20 to 100 ns are normal.

The pulse train c cannot be used directly to control a VCO. A filter circuit is required, or better still, an integrator which then delivers the VCO tuning voltage d. Every pulse in c corresponds to a voltage step in d. The VCO is now in the correct direction to be in tune but the steps are not as fine as might be desired. This leads to overshooting and consequent hunting about the lock frequency and this is characteristic of this type of phase detector.

Fig. 2 shows the relationships pertaining to the SH type. The reference frequency here is the saw-tooth waveform b. The pulses a set the time that the saw-tooth is sampled and then stored in an analog memory. In the lock condition, the output waveform c is filtered free of variations except under the possible conditions of noise contamination in the analog circuits.

It is easily forgotten that digital circuits also possess noise. It is present in the deviation that the actual flank times of a digital signal exhibit in respect to the theoretical correct times and must not be neglected in any PLL applications.

The basics of PLL can be looked up in the literature. From (5) a really simple explanation is given but which does not go into the HF techniques. A good over-view of all the HF applications is given in (1) where partial divisions, mixer principles and multiple loops (but not the SH detector) are treated. Finally, a precise treatment of theory and several examples of loops can be found in (6). The Motorola handbook (4) describes very early on, a PLL for the 2 m band. Its performance is not, however, adequate for current demands. The PLL basics will not then be gone into yet again in this article.

4. CONTROL TECHNIQUES

The local oscillator, frequency divider, reference oscillator and phase detector form a circuit (**fig. 3**) which, in spite of its internal digital signal techniques, has analog signals at its input and output. It is an electrical open-loop control system.

It is already known that at large diversions of the divided VCO frequency from that of the reference frequency, an FP detector delivers an output signal which exhibits an unambiguous directional sign whereas the signal amplitude is not so well defined. This tends to be proportional to the instantaneous phase difference. This sort of characteristic is known as dynamic non-linearity. It is already been seen that the output amplitude can only be changed in constant-time steps. These, in the language of control techniques, are known as dead periods. If the amplification is plotted against the frequency, with logarithmic

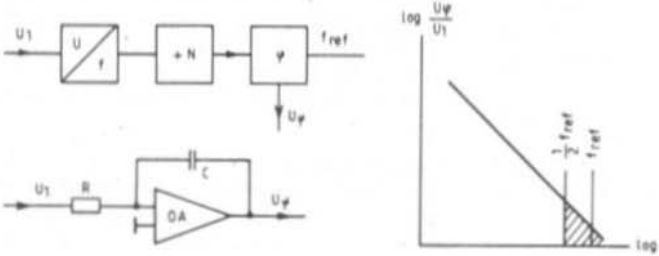

Fig. 3:
The control path, its analogue simulation and Bode diagram

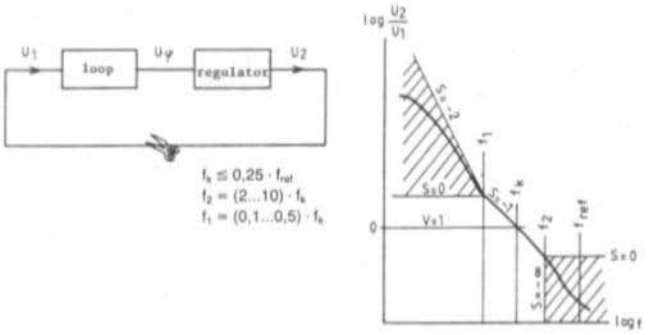

Fig. 4:
The control loop and its Bode diagram

axis having the same intervals for a decade, the Bode diagram of **fig. 3 (right)** will be obtained. This is necessary for the examination of the control system and represents an RC integrator circuit: –

$$RC = \frac{N}{U_B K_f}$$

where U_B = the IC's supply voltage
K_f = the VCO's modulation sensitivity (H_z/V)

When the frequency arrives in the vicinity of the reference frequency, the sampling function is more evident. According to Shannon's sampling theorem, after $f_{ref}/2$ there can be no certainty about the amplitude (shaded portion) and, initially, not about the phase either. It is clear that the system is functioning internally in a digital fashion.

One does not need to read thick books on control techniques to be able to dimension an electrical control system with dynamic non-linearity and dead period. Nevertheless, it is still not a trivial problem. Everything that is required is included in (6). An experimental analogue computer model is shown in **fig. 4** which can be constructed with a few operational amplifiers. In order to complete the loop only the controller in fig. 4 is necessary. This can sometimes be realized by a few resistors and capacitors and not more than one op-amp. The characteristics of the control loop can be determined as soon as the Bode diagram has been drawn. In order for it to be measured, the loop must be broken at a suitable place. In order that the control loop remains stable, certain points about the Bode diagram must be observed. The following represent the main criteria: –

- The critical frequency f_k at which the loop amplification goes through unity ($\log U_2/U_1 = 0$) must lie under $f_{ref}/4$.
- About the critical frequency, the rising frequency response must fall by -1. The limits of this range are at f_1 and f_2.
- Above f_2, the curve must lie in the shaded range. The steeper the slope falls, the better will be the suppression of transients from the phase detector.
- Under f_1 the curve must lie in the shaded region. If it lies in the vicinity of S = 0 (P controller), then in the lock condition the phase error will remain. If it lies near S = -2, the phase error is very small (I controller). The phase noise of the VCO has been effectively reduced.

The Bode diagram of the controller itself is not shown here. The difference that results from figs 3 and 4 is, in reality, a division because of the logarithmic presentation.

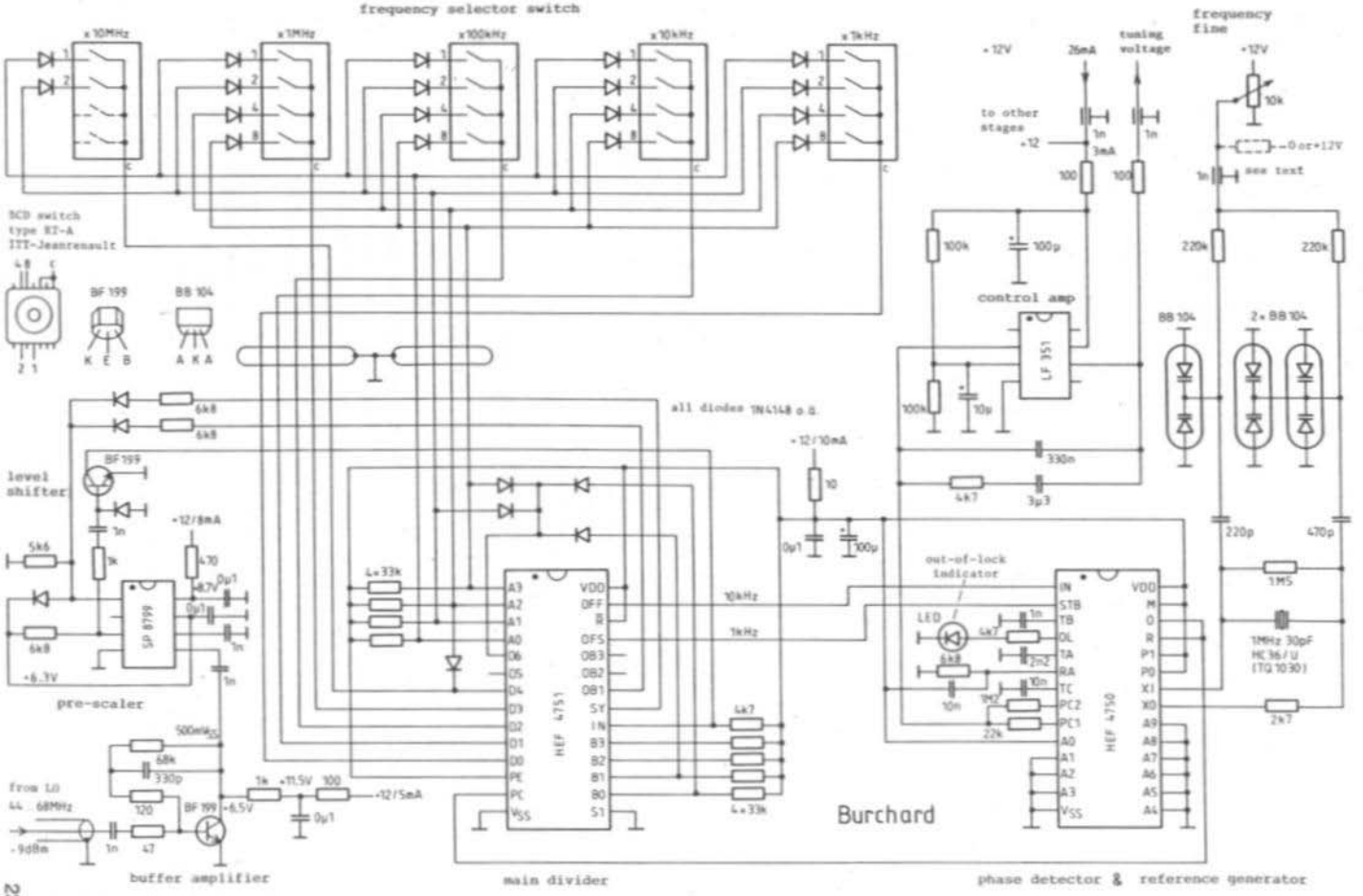

235 **Fig. 5: PLL circuit schematic**

The dimensions read into fig. 4 will result in a stable control loop. The coefficients can be selected to give an optimal lock condition or allow modulation to be effected. It will be noted that N/K_t will not stay constant over a large VCO frequency range. In the interest of stability, the smallest value should be dimensioned. Higher values will result in a larger lock time.

5. WHICH INTEGRATED CIRCUITS?

There are a variety of specialised chips with remarkable characteristics which have been developed for broadcast and television equipments. It must be borne in mind, however, that they could quickly disappear from the market owing to production limits or the series has been discontinued.

For this reason, it has been decided to use ICs which will probably have a long market life and also those that are familiar to the author.

The first one is the 4046 in the CMOS series. It contains two different phase detectors (EXOR and FP types) and a middling frequency VCO. The latter will not be of much interest even if the HC version is selected. The FP detector is usable for this project. Unfortunately, this IC has a very clumsy pin-out inasmuch that the input pin for the reference frequency is located next to the phase detector's output. It will be recalled that the FP output, for most of the time, is floating at a very high impedance and is very prone to the capacitive pick-up of interference signals.

The MC14568 has always been found to be very convenient. Besides having an FP detector it has a scaler for the reference frequency possessing the least significant quotients for the N divider. There is, however, a suitable matching N scaler (MC14569) with two additional decimal quotients. Incidently, all chips from the standard CMOS programme can be readily used with each other.

Even more highly integrated, and therefore in a smaller package, is the MC145156. This has a phase detector and a multi-stage N scaler together with a reference oscillator and control circuits for a dual-modulus divider. An FP output occurs only when an analogue switch and a differential amplifier are connected to it. That is a definite disadvantage!

The greatest complexity and flexibility is to be experienced by using the HEF4750. There are two phase detectors of the optimal FP and SH types with automatic, internal switching, a reference oscillator possessing a widely variable prescaler, and finally, a phase modulator. This has a companion IC (HEF4751) which provides 6 places of decimal scaling and which can be controlled by up to three pre-scalers of the dual-modulus type. It also provides for the IF offset. If a second IC of the same type is employed, the decimal places of the N divider following, will be doubled. That will function using partial division up to a frequency of 1 GHz. To understand all this completely, (7) must be studied. The price, DM 170.00 without prescaler, is very high. For it, one gets a 28 pin DIL package which requires plenty of space but little in the way of peripherals. Not all the functions will be required for this project but it has been chosen as being an expensive, but also the best solution.

6. THE CIRCUIT

The local oscillator (VCO) was taken from (3) and belongs to the frequency loop. It is not shown again here. It must be remembered that it was a varicap, tuned VCO working into two wideband stages. A small power of −9 dBm was coupled from the output to feed the PLL.

An oscillator, working directly on the desired frequency i.e. without multiplication or translation and used with a single-loop PLL and phase detector, yields the highest purity of output signal i.e. without prominent spurs. This quality is preserved by ensuring that digital signals are not allowed to encroach into the analogue parts of the circuit.

The circuit of **figure 5** starts off with a buffer

amplifier which also amplifies the −9 dBm input up to the middle of the input range of the pre-scaler. It also offers sufficient isolation for spurious signals at its output from returning into the loop. These spurious signals arise from capacitive coupling from the output of the pre-scaler and cannot be suppressed even by perfect screening. They must not, under any circumstances, appear at the −9 dBm buffer-amplifier input point, at a higher power than −80 dBm. This point should be checked. The return loss of the buffer stage amounts to some 25 to 35 dB. The negative feedback creates a virtual null point at the transistor base and also reduced its output impedance.

The SP8799 pre-scaler is of the dual-modulus type and divides by a factor of 10 or 11 according to the logic level at pin 1. A level shifter takes the pre-scaled frequency on to the main divider.

The HEF4751 now divides the signal down to the fast-reference frequency OFF (10 kHz) and the slow-reference frequency OFS (1 kHz). This occurs under the influence of a programme which is controlled automatically from the outputs of D0...D5 in which A0...A3 and B0...B3 inputs are read-in serially. A is the desired reception frequency in BCD-code negative logic, as set by the frequency selector. B is the IF in the same code. With the assistance of a few diodes and the B inputs, any weird IF-offset can be programmed. It is even more simple in this case, as the 1st IF is 40,000 kHz and the 1st decimal of the frequency selector is encompassed by 0, 1 or 2. The 4 can be fixed in A (i.e. diode between A2 and D4). D5 will only be necessary for the 6th decimal whilst D6 is tied up by the internal functioning of the IC.

The facility of frequency changing from a keyboard or a computer requires an interface which will take the A- and D-connections, according to function, to an external termination.

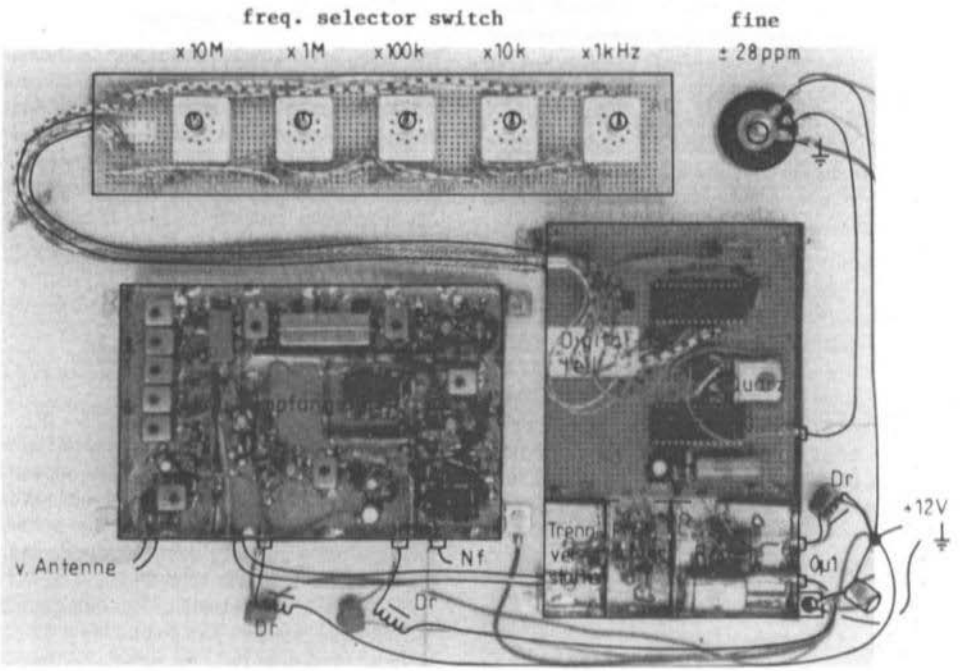

Fig. 6: Complete construction of PLL connected to SW receiver

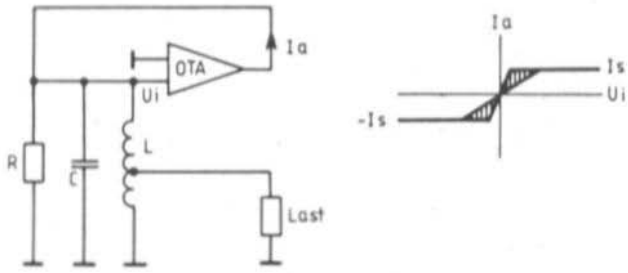

Fig. 7: Oscillator model

The phase detectors are embodied within the HEF4750. The FP type works with the 10 kHz reference thus giving a fast coarse tuning. The SH type works with the 1 kHz reference and tunes finely to the last decimal place. The change-over switching is automatically effected within the IC when the coarse tuning has reached ± 1 rad. The PC1-output remains then, in a quasi high condition and only the potential from PC2 tunes the remainder signal. Such "split-loop techniques" can require very complicated switching in other ICs. This arrangement requires only an extra resistance to PC2. The characteristics of the loop will, of course, vary along with the value of this resistance and two bode diagrams must be drawn. Only the second one needs to fulfil all stability criteria. Differences in the loop settling time of 1 : 100 are possible.

The interpolation was carried out in quite an unusual manner. In a digital system, a quasi continuous alteration can only be carried out in many small steps. If it is required to correct up to ± 10 Hz without using a second HF4751 it is only possible by varying the reference frequency. The 1 MHz crystal, however, can only be pulled over a range ± 28 ppm in this circuit. The functioning of a varicap must be considered as a combination of reactance control as well as a variation in capacitance since the AC voltage across it is considerable. If the nominal frequency of the crystal is set to the mid-travel of the potentiometer's rotor, then a resistance from the rotor to ground or to the +12 V rail is required. That depends upon the individual characteristics of the varicap and the potentiometer employed. The author's prototype required 22 kΩ to ground!

Other reference-frequency crystals in the range 10 kHz to 10 MHz are also possible but the reference-generator divider P must be set to divide by: 1, 2, 10 or 100, and A to divide by: 1, 2...1023).

In order to complete the loop, the control is effected with the operational amplifier LF351. This is so connected that the lock-in time lies between 100 and 200 ms which is very suitable for a hand-operated tuning system.

The author's prototype construction is shown in **fig. 6.** The HF-sensitive circuits are constructed on Minimount and the digital circuits on Veroboard. The complete assembly was packaged in a screened housing which had compartments for buffer amplifier, the pre-scaler and the controller. The shortwave receiver (3) was then suitably connected.

7. THE PAINFUL PHASE-NOISE

The quality of a generated signal is given by the ratio of its amplitude to that of the undesired spurious product signals. This will not include purely harmonically related signals. The spurious products arise primarily from thermal effects in the tuned circuit and as both thermal and flicker noise in the active elements. The latter amplify the spurious products and deform them through inherent non-linearity. An ideal model, for example, would have a large wanted-signal vector and a very small noise component whose

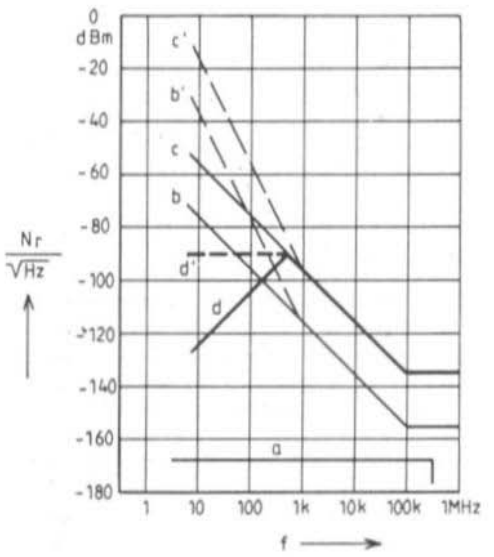

Fig. 8:
Sideband phase noise
a thermal noise of tuned circuit
b phase noise due to parametric effects in the active element and tuning diodes under the influence of white noise
c phase noise amplified by 20 dB
d reduction of phase noise by the PLL in the presents of 1/f noise under 1 kHz

magnitude and direction varies continuously in a random manner. These noise vectors can be thought of as being split into a vector pair, one representing amplitude modulation and the other phase modulation – half the total noise energy being invested in each.

In order to see how a real oscillator behaves with this concept, refer to the oscillator of **fig. 7.** The tuned circuit LCR has its losses replenished by the amplifier. This is represented by the curve on the right. The output current is constant, apart from a steep linear portion which is dependent upon the polarity of the input voltage. The input and output impedances are both desirably high. Such an oscillator can be realized by using an Operational Transconductance Amplifier (OTA) or a differential amplifier. The load is matched by the suitable tapping of inductor L to resistor R.

This means that dynamic resistance is R/2 and the Q is half that of the unloaded Q. I_s is so chosen that there is a power output in the load of 0 dBm i.e. 1 mW – quite a normal output for an oscillator of this project.

The thermal noise from R appears at the load as a bandpass noise a, in **fig. 8**. The turn-over frequencies depend, of course, upon the Q of the tuned circuit. Its magnitude can be calculated in accordance with Boltzmann and does not play a large role in actual oscillators. Passing the noise through the amplifier will saturate the AM noise and suppress its AM component by limiting action. Half the noise will be retuned by the feedback as phase noise modulation. But this is also so small that its inclusion in fig. 8 is not warranted. Even when the noise source from the amplifier is inserted in series with the amplifier input and whose magnitude is several times that of R's thermal noise, the total effect is still negligible.

There must then be another mechanism at work. This is to be found in the parametric effects of the tuned-circuit's reactance and the deficiencies inherent in the amplifier. The addition of a voltage-dependent capacitance contributes heavily to this effect. In the oscillator of (3) the thermal noise in the 10 kΩ resistor in series with the varicap is shown in fig. 8 curve b, as a sideband noise. Similarly, the base resistance and diffusion resistance of a transistor generates noise voltages in the inherent base-emitter capacitance. The white-noise sidebands of such a source fall away linearly since the magnitude of the spectral lines are dependent upon the phase deviation which is, in turn, a function of the deviation ratio as follows:

$$\Delta\varphi = \frac{\Delta F}{f}$$

where ΔF is the frequency deviation and f is the modulation frequency. The inclusion of an active element possessing a large flicker noise significantly increases the sideband amplitudes in the immediate vicinity of the carrier thus giving rise to curve b'.

Although measures can be taken to improve the sideband noise (use a transistor with a better noise figure, control saturation, high-Q tuned circuits, small parametric reactances, noise matching etc.) they are difficult to implement in practice. In particular, at the higher frequencies the availability of suitable transistors become smaller.

The theme of noise matching and parametric reactances, over-driven stages, is still very much a closed subject. The aforementioned 10 kΩ resistor, however, can be replaced with an RFC of 4.7 to 10 μH giving rise to an immediate noise improvement of some 5 dB.

Following the signal's amplification by 20 dB in an LO-driver amplifier (which should have a low noise figure) the curve of c and c' of fig. 8 is constructed.

What can now be improved in the phase locked loop? That is, theoretically, easy to answer. The improvements are exactly in accordance with the amplification of the open loop of fig. 4 in the absence of additional noise or spurious signals in the control loop. The improvement is concerned then, only with the frequency range below f_k! It is completely out of the question that some sort of improvement takes place where the adjacent channel is located! The LO must be inherently noise-free over the frequency occupied by the adjacent channel.

The PLL, however, prevents long-term drift, reduces flicker noise and microphony to a few hundred Hertz, in this example. It would be a mistake to assume that the ills of a poorly designed and constructed oscillator can be cured by the phase locked loop. As shown in curve d or d' in fig. 8, from the original noise "trumpet" the PLL introduces a noise pedestal which may be displayed on a high-resolution spectrum analyzer.

The loop is not free from noise and other spurious sources. Phase detectors of the EXOR- and RS-FF-type deliver, at least, spurious signals at f_{ref} and harmonics thereof. This gives rise to spectral lines in the output which fall directly into the adjacent channels. The FP type gives rise to burst signals which are of a similar nature to flicker noise. Finally, the reference frequency is not free of phase noise and also, the noise generated in the loop operational-amplifier noise cannot be neglected. All this must be taken into account when the loop gain is to be equated. The SH phase detector with a zero-gain design (not mentioned here) should always be considered.

Poor isolation of inputs from outputs of digital circuits, clumsy pin-outs (as in the 4046) and power leads can also deteriorate the output signal of the SH phase detector. Then sometimes, only the reduction in f_k will reduce the spectral lines from appearing in the output. That, of course, results in a smaller loop gain. Oscillators which are to be phase modulated, require a PLL which does not influence the loop in the modulation frequency range. f_k must therefore be low enough to ensure this. The IC used here (HEF4750) can be usefully modulated in the SH phase detector, along with the oscillator, in order that no control voltage is generated. That is an interesting feature of which no use is made of here.

8. MEASUREMENTS

These are important to ensure that the design objectives have, in fact, been achieved. The results for the construction of fig. 6 are documented in the manner of those in (3). A depiction of the sideband noise present in the adjacent channel is not included, since it cannot be differentiated from the oscillator in the absence of the PLL.

The reaction of the loop to sudden changes in the reference is shown in the traces of **figs. 9 and 10.** The output of PC1 (FP detector) is shown uppermost and the output of the PC2 (SH detector) is shown in the lowest trace. The middle trace is the PLL tuning voltage. The program step in fig. 9 is 10 MHz. This is accomplished using a reed-relay contact which switches the first decimal place from 2 to 1. After 60 ms, the PC1 has covered the F range and ripple in the tuning voltage can be clearly seen as the instantaneous transitions to final tune occur. In the P range,

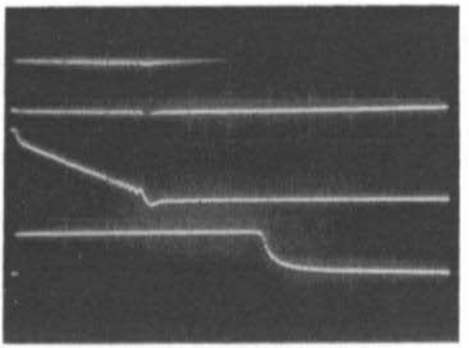

Fig. 9:
Reactions to a 10 MHz frequency step (65 to 55 MHz)
Y1: PC1 output 5 V/div
Y2: Tuning voltage 2 V/div
Y3: PC2 output 5 V/div
X: 20 ms/div

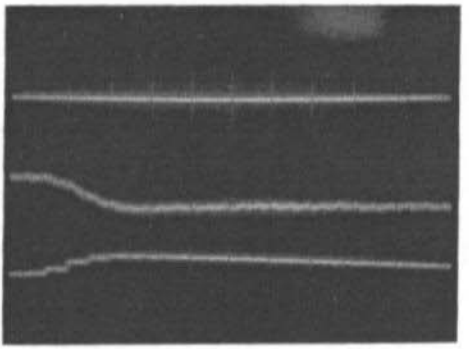

Fig. 10:
Reactions to a 10 kHz frequency step (60.020 to 60.010 MHz)
Y1: PC1 output 5 V/div
Y2: Tuning voltage 5 mV/div
Y3: PC2 output 1 V/div
X: 2 ms/div
Y2 and Y3 are AC-coupled which explains the slight slope!

the pulse width in the PC1 varies continuously to smaller values (the smallest are lost in the trace width) until the final tune point of PC2 is achieved after 110 ms. PC1 remains open and the remaining step adjustment will be carried out by PC2. This takes 140 ms. The 10 kHz steps (fig. 10) do not require the involvement of PC1. PC2 achieves this step in just 5 ms. The considerably higher oscilloscope Y2 and Y3 channel sensitivities should be noted in this presentation. The ripple seen on these traces is not necessarily produced by the signal under observation. The open construction allows signals from the digital section to be picked up directly by the oscilloscope probe.

A reference for the spurious phase deviation is the voltage at PC2 in the rest (tuned) condition. This is shown in **fig. 11**, upper trace. The LO is received on a calibrated receiver having a 5 ms de-emphasis. This corresponds to a ØM demodulation with a lower limit frequency of 30 Hz. The trace photograph is shown in fig. 11, lower trace. Both curves are shown instantaneously over the same time period and show a great degree of conformity but they are not congruent. They are taken, actually, from two different points in the loop and confirm that there are other noise sources to be reckoned with. The lower trace also contains the phase noise from the oscillator and demodulator in the laboratory receiver. From the two traces, it can be estimated that frequencies under 20 Hz and over 200 Hz do not play any important role. The noise pedestal conforms approximately to that of fig. 8 d'. An

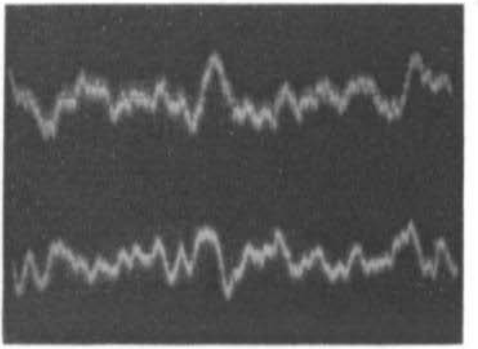

Fig. 11:
PLL phase noise
Y1: PC2 output 5 mV/div
Y2: ØM-output from laboratory receiver
30 Hz...30 kHz
2 rad/div
X: 20 ms/div

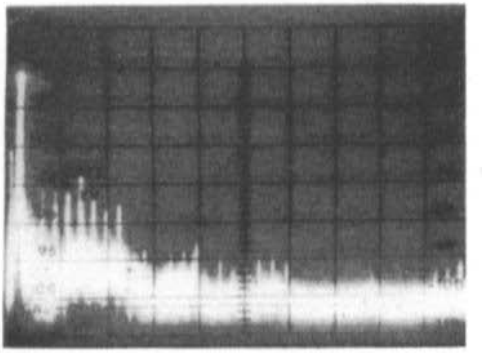

Fig. 12:
Spurious signals on the frequency selector line
Y: 10 dB/div, the 200 kHz CAL-line represents 45 dBμV
X: 20 MHz/div, zero marks, 0...200 MHz.
Analyzer bandwidth 200 kHz, video filter 10 kHz

LF spectrum analyzer would be able to confirm this more exactly.

Digital signals are potential HF-interference sources having considerable energy in the short-wave region. They cannot be allowed to roam around freely as in some unsatisfactorily screened computers. In this case, they are not only an environmental menace but are also suicidal for the project! **Fig. 12** shows the interference spectrum existing on the line to the frequency-selector switch. It was obtained using a series resistor of 5 kΩ from the 50 Ω input socket of the analyzer. This resistor prevents interference with the digital workings and reduces the signal to be measured by some 40 dB. To conform with interference measurement practice, the units chosen are dB rel 1 μV. Everything which rises above the CAL line by more than 15 dB is inadmissable because it is over the interference grade N. Everything which is visible on the trace is capable of causing interference to local receivers. The frequency-selector switch and its cable must therefore, be carefully screened. The cable screening may be seen in fig. 6.

There is one method by which continuous interference can be reduced in a single blow. The divider HEF4751 can be so operated that its frequency programming to PC is taken to the internal memory where it awaits the sampling signal. It then requires a switch, which can only be described as 'enter', to complete the operation.

All the other digital signals tumble around in the screened compartments and, with judicious use of RFCs and feed-thro' capacitors, are not allowed to cause any trouble. Spurious-signal loops are avoided by using RFCs in the +12 V supply line and the tuning leads, as may be seen in fig. 6. These comprise twin-holed ferrite beads with 4 turns of multi-strand wire. Each RFC need only have an inductance of a few μH.

9. REFERENCES

(1) The ARRL 1986 Handbook
Radio Frequency Synthesizers, chapter 10, pp 10-8...10-18
The American Radio Relay League, Newington CT

(2) H. Böhnhoff (1956)
H & B Taschenbuch: Elektrische und wärmetechnische Messungen
Der Fallbügelregler, S. 93
Kramer & Co, Frankfurt/M

(3) D. Burchard: Shortwave Reception – Based on the Thirties Principles. Part 1 and Part 2
VHF COMMUNICATIONS, Vol. 22, Ed.1/1990, P. 23 - 30.
Ed. 2/1990, P. 70 -76

(4) C. Crook et.al. (1974)
McMOS Handbook, 2nd edition, chapter 10, pp 10-1...10-10
Motorola Semiconductors, Switzerland

(5) D. Lancaster (1980):
Das CMOS-Kochbuch, 1. Aufl., Kap. 7, S. 7-26...7-38
IWT-Verlag, Vaterstetten

(6) U. Tietze & Ch. Schenk (1980):
Halbleiter-Schaltungstechnik, 5. Aufl., Kap. 26, S. 688...714, Elektronische Regler
Springer-Verlag, Berlin

(7) Integrierte Digitalschaltungen LOCMOS-Reihe HEF 4000 B
Valvo Handbuch
Valvo/Philips, Hamburg

G. Tomassetti, I 4 BER and S. Mariotti, IK 4 JGD

A "New" Feed for the 3 cm Band

(Presented at Microwave Conference in Bologna, May 1989)

A back-fire feed for small dishes is often chosen because of its greater practicality than the traditional pyramidal horn particularly when mountain-topping operations are contemplated. Among the various designs to be found in the literature, the feed chosen is rarely used by amateurs in spite of its mechanical simplicity and electrical attractiveness. It is therefore presented as a re-discovered feed method despite its having been published as early as 1955 in the ARRL-Antenna Handbook. The dimensions for a 9400 MHz version are given by Henney in his Radio Engineering Handbook (1959). The design does in fact suggest a much earlier military (RADAR) origin. (Ed. It was also published in VHF COMMUNICATIONS 2/79 by DK2VF and DJ1CR with very similar dimensions to the one described here.)

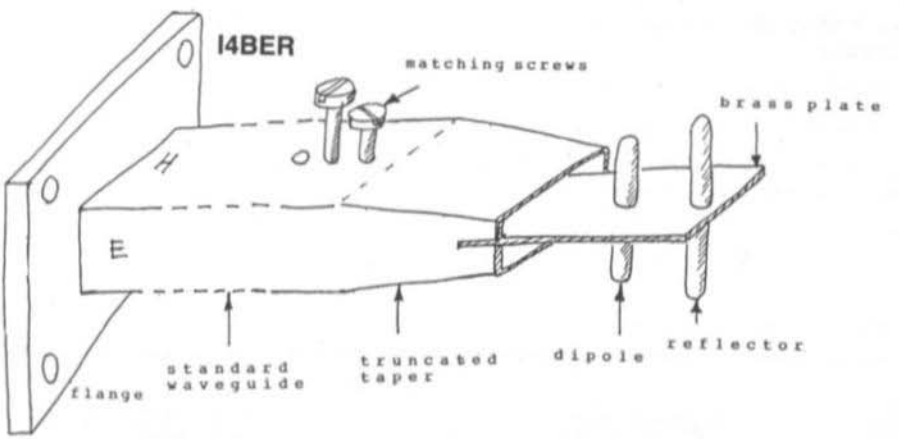

Fig. 1: Parabolic reflector exciter (length shortened in dia.) together with matching screws and WG flansh

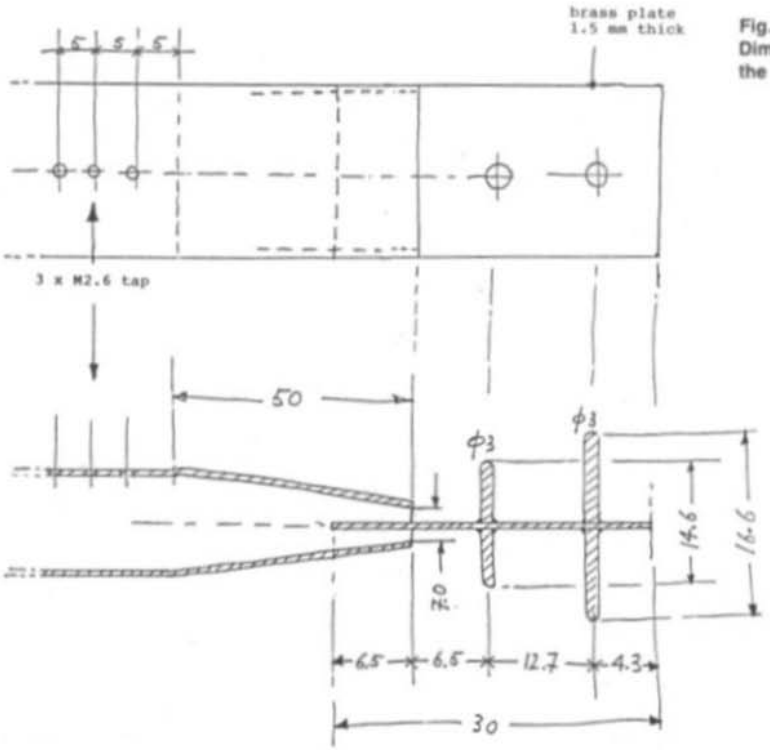

Fig. 2:
Dimensions of exciter for the 10 GHz amateur band

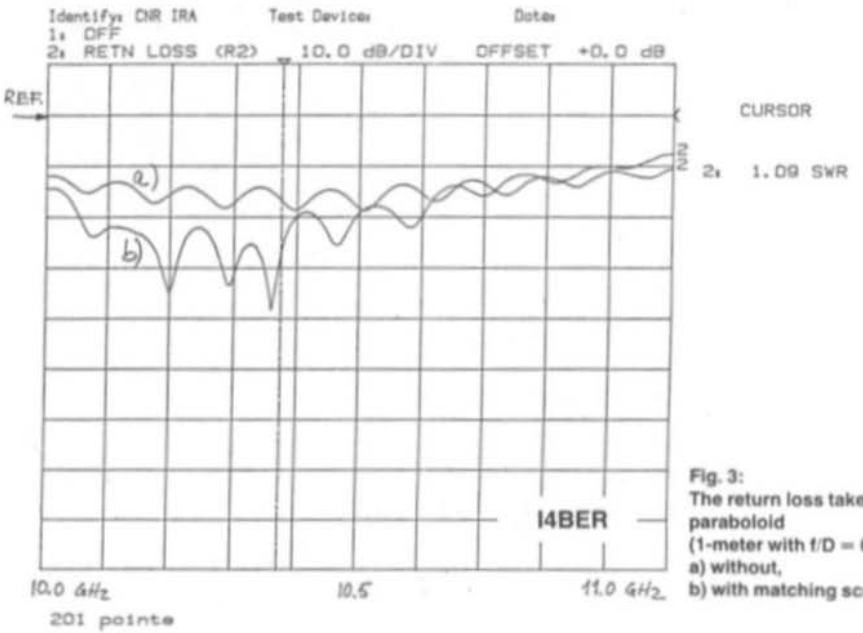

Fig. 3:
The return loss taken in the test paraboloid
(1-meter with f/D = 0.44)
a) without,
b) with matching screws

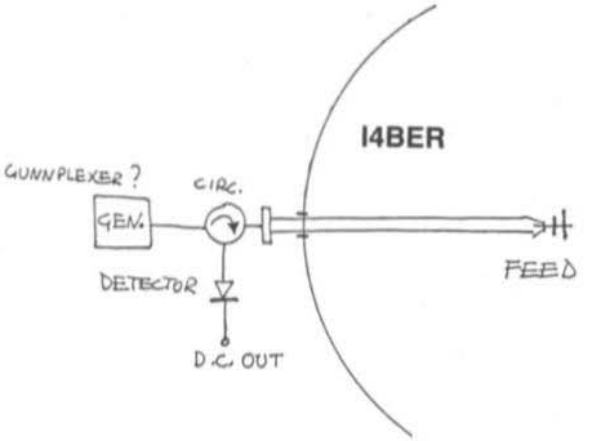

Fig. 4:
Arrangement for indicating and optimising the return loss

The feed consists of a length of standard waveguide with a flansh at one end and a truncated taper at the other end. A 1.5 mm brass plate is slotted into the end of the taper. This plate carries a two-element Yagi in a plane parallel to the electrical field of the waveguide's dominant TE_{10} mode. This antenna reflects most of the energy emanating from the waveguide back into the inner surface of the reflector (**fig. 1**). Silver solder is used to fix the plate to the waveguide and also the antenna rods to the brass plate. The dimensions of the plate assembly are given in **fig. 2**.

After preliminary testing, an improved performance was obtained by replacing the reflector rod with a disc of brass having a diameter equal to the width of the waveguide (i.e. 28 mm). It is advantageous if this disc is arranged to be adjustable over a range of a few mm in the plane of the waveguide in order to optimise the dish illumination. The dimensions for this antenna feed were obtained by a linear scale down of the dimensions given in the original design. The effectiveness of this approach may be judged by the curves of **fig. 3**. The return loss in the absence of waveguide matching screws is about 15 dB over the range 10 - 11 GHz. The introduction of the matching screws enables the return loss to be improved to more than 30 dB over a limited sector of the band as shown in curve 3b.

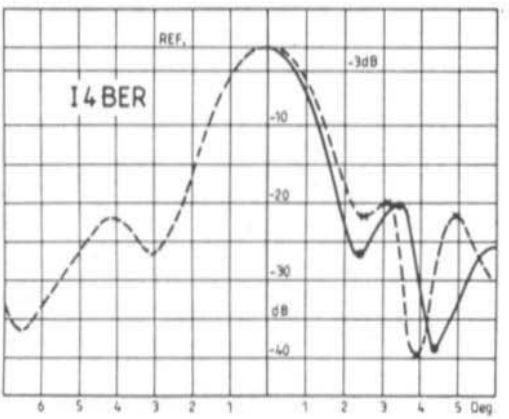

Fig. 5:
Polar diagram of the test antenna with the subject feed showing beamwidth of approx. 2°

A cheap and practical arrangement for matching the feed is suggested in **fig. 4**. The circulator can be replaced by a directional coupler with suitable coupling and directivity specifications. In any event, the aim is to minimise the power (monitored as the DC flowing from the detector) reflected by the feed.

The azimuth and elevation polar plot of a 1 m dish with a 0.44 f/D ratio and illuminated by the subject feed arrangement is shown in **fig. 5**. The data for the plot was taken by measuring the power received from a beacon atop a 25 m tower some 350 m away and displayed on an HP spectrum analyzer. The data is believed to be accurate within ± 1 dB and ± 0.5 degrees. The illumination tapering was not measured as it was considered to be too difficult. However, if the side-lobe level, predicted by theory, is correct, a tapering in the order of 6 - 10 dB at the edge of the dish is to be expected. This is probably in order for an amateur tropo location.

The measured beamwidth of the 1-meter test dish turns out to be just below the 2 degree mark in both the E and the H plane thus conforming with the predicted figure. A comparison of the received power when feeding the same dish with a standard horn and then the subject feed, showed a deterioration of 0.5 dB for the latter configuration – well within the accepted measurement error.

Wolfgang Borschel, DK 2 DO

Tropospheric Forward-Scatter Propagation

Forward-scatter propagation is used by amateurs wishing to participate in contacts which extend well over the normal distances expected for that band. In the same manner as the well known meteor trail propagation, both means rely upon the scatter phenomena for their operation. The mechanism upon which forward-scatter radio propagation relies, will be considered briefly in this article together with some comments based upon personal observations.

The mechanism of this mode of communication is explained in **fig. 1**.

1. SCATTER PROPAGATION

This mode of propagation utilizes the random dielectric constant distribution of many small elements (**fig. 2**) which are formed by turbulance in the atmosphere, to diffract the main radio beam. The resulting discontinuity scatters a certain portion of it downwards towards the receiving antenna. As the diagram of fig. 1 shows, only a very small fraction of the energy intercepted by the scatter volume is deflected earthward, the main beam continuing on into space without any major refraction. The intensity of the scatter effect is dependent upon the local variations (turbulence) of the elemental dielectric constant. This activity is more likely to be at its most intensive where the weather fluctuations are at their most extreme, namely the troposphere.

The whole process of forward-scatter propagation is analogous to that observed when a searchlight beam is directed into the air. It is most readily apparent when it shines through cloud, smoke, fog, etc, even though only a tiny fraction of the beam is diffracted into the observer's eye.

The part of the troposhere which is responsible for refracting the energy downward, for any given path, is known as the scatter volume. This is depicted in fig. 1, where it may be seen as the filled-in area of the cross-sectional diagram. The usable signal is formed through the addition of all the refracted components from differing parts of the scatter volume which impinge upon the receiving antenna's surface. This implies that the transit time is not constant and the

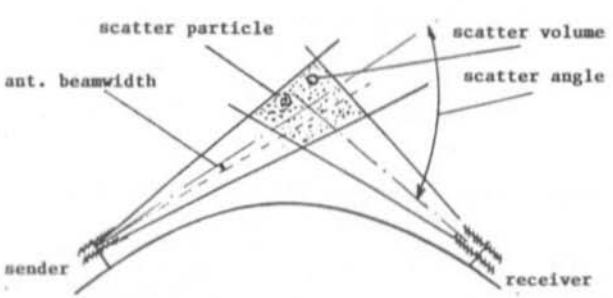

Fig. 1: The mechanism of tropospheric communication

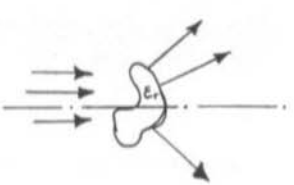

Fig. 2: An elemental particle in the scatter volume

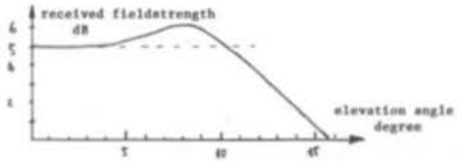

Bild 3: Observed dependence of the received field strength upon the receiver-antenna's elevation angle

resulting phase variations give rise to rapid fading and Hall effects. The path attenuation, to be expected with the forward scatter mode of propagation, rises rapidly (exponentially) with the angle of scatter and also with the frequency. This means, of course, that there will be a much greater path attenuation on 70 cm – than on the 2 m-band.

As a further consequence of the variation in path transit-time, selective fading puts a restriction on the permissible channel bandwidth. The mode is not suitable for any wider modulation mode than SSB (ed: although as many as 132 SSB channels are in simultaneous use over individual, commercial and military, frequency division, MUX, forward-scatter links!).

2. FORWARD-SCATTER WORKING

The increasing contamination of the atmosphere through dust particles, actually assists this mode of propagation. Observations over many years at the author's station, have not, however, revealed the exact correlation of the various factors affecting the propagation, such as, the weather, air temperature, scatter volume constituency as well as the elemental dielectric constants. Of course, it is not realistic for an amateur station to expect any exact results from investigations into the scatter volume, its dielectric constant and its constituency. It may be presumed, however, that elements other than air must be involved for the degree of refractions experienced, and that these could well result from the emissions from heavy industry into the atmosphere.

The assumption can be taken a step further by implicating sulphur, oxides of various kinds as well as dust particles, to account for the type of refraction involved in this mode of propagation. Forward-scatter propagation is particularly good over large centres of industry – the author lives in the Ruhr industrial area – and can be experienced during the whole of the year. Weather conditions are a dominating influence: rain washes the dust from the atmosphere thus deteriorating the scatter volume constituency whilst thermal effects seem to favour it.

Amateurs living in the industrial zone itself will find it difficult to utilise this method of propagation because the scatter angle is very large.

Pre-requisites for this mode of propagation are; high antenna gains, very good receive-system sensitivity and high transmitter output power. The scatter angle must be very small and the shoot angle (**fig. 3**) appears to have an optimum which lies between 5° and 15° depending upon the prevailing characteristics of the scatter volume. It may be seen that using low beamwidth antennas, the received signal strength increases slightly before it drops away sharply with the increasing angle of elevation. It appears to be the case, that forward-scatter propagation is more favourable over heavy industrial regions than elsewhere.

3. REFERENCES

(1) Gerber, Peter, HB 9 BNI:
The Doppler Effect over Radio Links using Active or Passive Reflectors
VHF COMMUNICATIONS, Vol. 19, Ed. 2/1987, P. 88 - 91

(2) Weiner, Karl, DJ 9 HO: UHF-Applikation: UKW-Wellenausbreitung.
F 1.2.4 Streuung von Funkwellen.
Weiner-Verlag

(3) Borschel, Wolfgang, DK 2 DO:
Diagrams that allow one to easily determine the Sensitivity of Receive Systems using Solar Noise. VHF COMMUNICATIONS; Vol. 16, Ed. 4/1984, P. 247 - 250

Jochen Dreier, DG 8 SG

Simple Improvements to the DK 2 VF Microstrip Directional Coupler

Some amateurs will remember the 2 m (DK2VF 001) and the 70 cm (DK2VF 002) directional couplers which were published in VHF COMMUNICATIONS 2/1971. It was remarked at the time, that the directivity was poor (14 dB) and its main-line VSWR was rather high at 1.5 : 1. A recent look at the design prompted the question: why should it be so bad and how can it be improved?

1. ANALYSIS

A theoretical analysis (1), (3) of the main-line – which has a better matching according to the magnitude of the coupling loss i.e. little mutual coupling – was found to be in accordance with

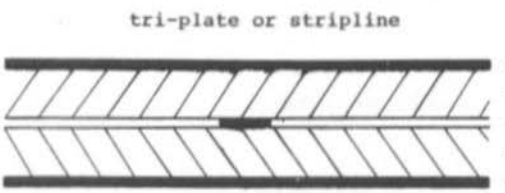

Fig. 1:
Tri-plate or stripline

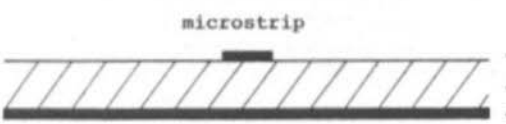

Fig. 2:
Micro-strip

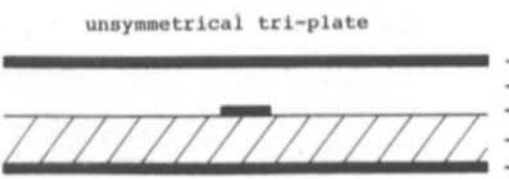

Fig. 3:
Unsymmetrical tri-plate

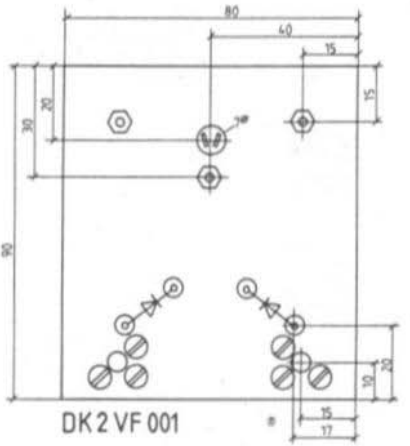

Fig. 4: Supplementary board to the DK2VF 001

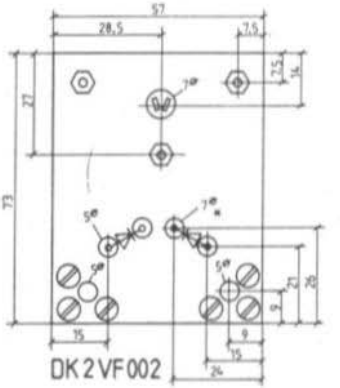

Fig. 5: Supplementary board to the DK2VF 002

the measured data but that it was too narrow. The question was now: how can the lines on the existing PCB be made wider, or, the other way round: how can the existing lines be rendered wide enough?

The solution lay in the use of a tri-plate (**fig. 1**). This tri-plate, or stripline, is a symmetrical conductor, as opposed to microstrip (**fig. 2**), which is often incorrectly referred to as stripline. Tri-plate has a higher capacitance and is therefore a lower characteristic-impedance line.

A further theoretical analysis of an unsymmetrical stripline (**fig. 3**), shows the encouraging result, that it is in fact completely (electrically) symmetrical!

One difference should be mentioned, however, the line will have a higher coupling loss but this

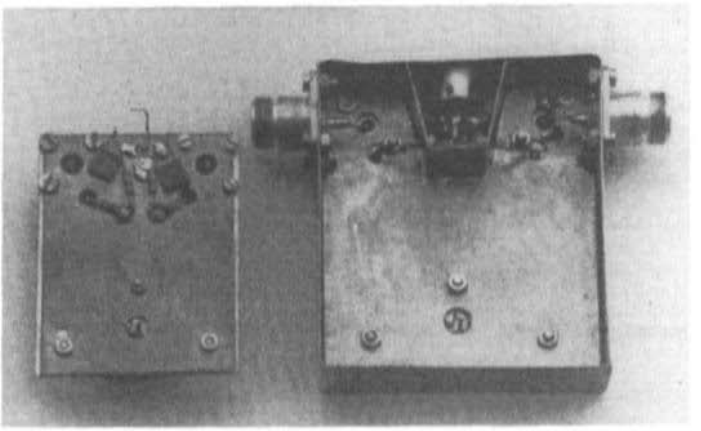

Fig. 6:
Both modified couplers

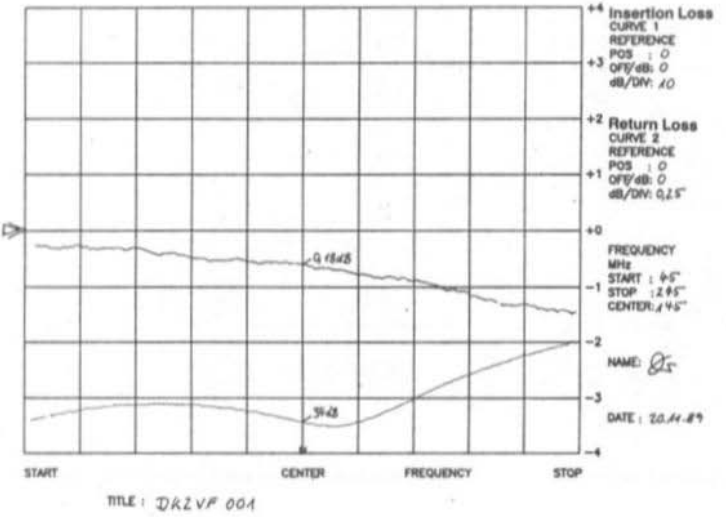

Fig. 7: Sweep traces of the modified DK2VF 001 coupler

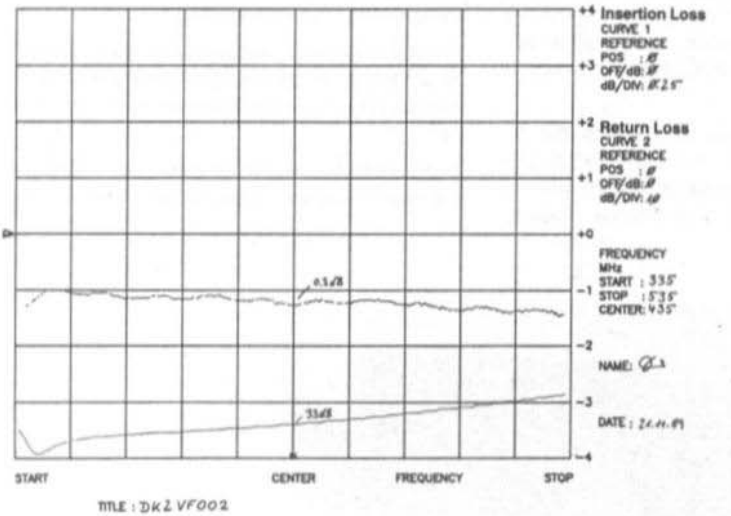

Fig. 8: Sweep traces of the modified DK 2 VF 002 coupler

will pose no problems for the majority of applications.

Test results on a tri-plate, modified DK2VF 002 board measured with an HP 8754A and using precision terminations, were as follows:–

Main-line VSWR: 1.05
Main-line insertion loss: 0.3 dB
Directivity: 30 dB

2. MODIFICATION DETAILS

Materials:
Single-sided, glass-epoxy board, 1.5 mm thick and the same size as the coupler
2 Chip resistors 56 Ω, RC 01, MCR 18 or equiv.

Method:
Holes are drilled in the appropriate places for the components (connectors, diodes, decoupling capacitors, termination resistors, screws) as shown in the drawings of **fig. 4** and **fig. 5**.

The existing potentiometer, which is not suitable for these frequencies, is replaced by two inexpensive chip resistors. The coupled line is physically separated in order to prevent cross-coupling. Perhaps a single chip resistor of 27 Ω or 33 Ω can be used if the line is not split but the author has not tried this.

After the potentiometer and diodes have been soldered in (disc capacitors can remain), the board is completely cleaned of residual solder in order that there is no air remaining between the boards. The drilled, additional board, is then screwed on to the old coupler in order that it holds the tri-plate with the ground-plane facing outward. The diodes are re-soldered in and the modification is thereby completed.

A modified coupler may be seen in **fig. 6. Figures 7 (2 m) and 8 (70 cm)** show sweep traces for both the directivity and the coupling loss of the modified coupler.

It will give me great pleasure if my article has resurrected the reputation of the DK2VF-coupler. Any comments will be welcomed.

3. REFERENCES

(1) Hupfer, K., DJ 1 EE:
Striplines for VHF and UHF
VHF COMMUNICATIONS Vol. 3, Ed. 4/1971, P. 207 - 216

(2) Meinke, Gundlach:
Taschenbuch der Hochfrequenztechnik

(3) NTZ-Archiv, S. 413

(4) cq-DL 5/84, S. 212

(5) Elektronik 8/89, S. 118 - 121

(6) UKW-BERICHTE 1/64, S. 47 - 56

(7) SCOMPACT, Vers. 1.95

(8) Stadler, E., DG 7 GK:
The Directional Coupler, Function and Use
VHF COMMUNICATIONS Vol. 17, Ed. 3/1985, P. 178 - 184

MATERIAL PRICE LIST OF EQUIPMENT

DJ4LB	**A Universal Sound-Vision Unit for FM-ATV Transmitters**	**Art.No.**	**Ed. 2/90**
PC-Board	DJ4LB 010 Europe format (100 x 160 mm)	6115	DM 35.00
DC9DO	**SAT-X Receiver for the Satellite IF Band 900 - 1700 MHz**	**Art.No.**	**Ed. 1/90**
DC9DO 001	PC-Board	6364	DM 38.00
DC9DO 001	Special components: BFQ 69, 3 x MSA 0304, 7805, SL 1452, TL 082, SO42P, 5 x BB505B, BB405B, 5 x 1N4151, Z8V2, Z5V1, LED red; trimmpoti (horiz): 100 Ω, 470 Ω, 47 k, (upright): 2 x 47 k, 4.7 k, foil trimmer 3 x, 4 mm coil former with ferrite core 3 x, CuL wire, silvered wire; RFCs: 33 µH, 22 µH, 15 µH, 3 x 100 µH; tin-plate box	6365	DM 120.00
DF9DA	**Compact METEOSAT Converter**	**Art.No.**	**Ed. 1/1990**
DF9DA 001	kit with all components	6510	DM 395.00
	ready-to-operate module	3029	DM 575.00
DF9DA 002	**Compact Weather-Satellite FM Receiver**		**Ed. 2/1990**
DF9DA 002	kit with all components, with 1 crystal for 137.5 MHz	6511	DM 445.00
	Receive crystal for 134.0 MHz (METEOSAT-ch. 2)	6512	DM 34.00
	Receive crystal for 137.62 MHz (NOAA-9 and 11)	6513	DM 34.00
	Ready-to-operate module (with 3 crystals)	3310	DM 890.00
YT3MV	**DSP Computer for Radio Amateur Applications**		**Ed. 2/1988, 1 + 2/1989**
Set of PCBs,	**progr. EPROM with authentic documentation** Contains: PCBs YT3MV 003 (bus), 004, 005, 006 (4 x), 007, 008 and 009; a programmed EPROM (operating system with Compiler, Editor), a set of copies of all diagrams and component lay-out plans (in A4), the operating-system manual.	6004	DM 599.00
YT3MV 010	**Interface for KR-5600 Rotators** PCB, progr. EPROM, together with A4 copies of circuit schematics and comp. loc. plans	6003	**Ed. 1+2/1989** DM 100.00
User software	Several software packages complete with image examples on 3.5" floppy disks	6002	**Ed. 3+4/1989 2+3/1990** DM 145.00

DCØDA	**10 GHz Transverter System "microline 3"**		**Ed. 2 + 3/89**
XLO-1	**Oscillator**		**Ed. 2/89**
Kit	contains all original components listed in chapter 2.3.	6601	DM 178.00
Module	ready-to-operate	6600	DM 248.00
Option 01	with stab. crystal (TK 10 ppm), temp.-compensation	S 3031	DM 314.00
XRM-1	**Receive mixer**		**Ed. 3/89**
Kit	Contains all original components listed in chapter 3.3.	6603	DM 345.00
Module	ready-to-operate	S 3032	DM 498.00
XTM-1	**Transmit mixer**		**Ed. 3/89**
Kit	Contains all original components listed in chapter 4.3.	6605	DM 355.00
Module	ready-to-operate 100 mW	S 3033	DM 525.00
Option 01	200 mW	S 3034	DM 598.00
Original Johannson trimming tool for μW trimmer		**6607**	**DM 18.50**

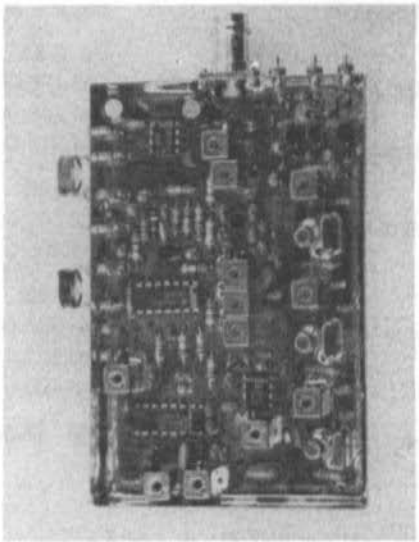

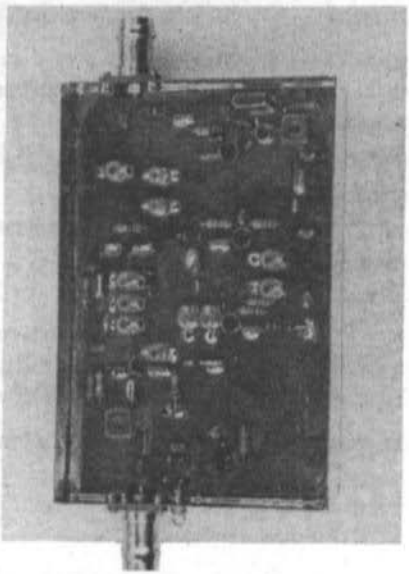

A new METEOSAT converter as a compact kit, Description in VHF COMMUNICATIONS 1/1990

- Input frequencies: 1691.0 and 1694.5 MHz
- Intermediate frequencies: 137.5 and 134.0 MHz
- NF = 1.7 dB (typ); G = 26 dB (typ)
- Operation voltage 12 - 14 V, approx. 80 mA
- Dimensions (mm): 111 x 74 x 30 and BNC sockets

The matching weather-satellite receiver, Description in VHF COMMUNICATIONS 2/1990

- 3 channels: 134.0/137.5 and 137.62 MHz
- Sufficient sensitivity for direct NOAA reception on 137.5 and 137.62 MHz
- Operation voltage 12 - 14 V; Connections for loudspeaker, S-meter, channel-switch
- Dimensions (mm): 111 x 74 x 30 and BNC socket

Special offer (in stock)	**Art.No.**	**Price**
Converter, kit with all components DF9DA 001	6510	DM 395.00
Converter, ready-to-operate module	3029	DM 575.00
Receiver, kit with all components DF9DA 002 (with 1 crystal)	6511	DM 445.00
Crystal for 134.0 MHz	6512	DM 34.00
Crystal for 137.62 MHz	6513	DM 34.00
Receiver, ready-to-operate module (with 3 crystals)	3310	DM 890.00
The matching pre-amplifier:		
Mast pre-amplifier, ready-to-operate (G = 38 dB)	6120	DM 445.00

Plastic Binders for VHF COMMUNICATIONS

- Attractive plastic covered in VHF blue
- Accepts up to 12 editions (three volumes)
- Allows any required copy to be found easily
- Keeps the XYL happy and contented
- Will be sent anywhere in the world for DM 10.00 including surface mail

Please order your binder via the national representative or directly from UKW-BERICHTE, Terry Bittan OHG (see below)

Prices for VHF COMMUNICATIONS

Subscription	Volume	Individual copy
VHF COMMUNICATIONS 1991	**each DM 35.00**	**each DM 10.00**
VHF COMMUNICATIONS 1990	each DM 27.00	each DM 7.50
VHF COMMUNICATIONS 1988 to 1989	each DM 25.00	each DM 7.50
VHF COMMUNICATIONS 1986 to 1987	each DM 24.00	each DM 7.00
VHF COMMUNICATIONS 1985	DM 20.00	each DM 6.00
VHF COMMUNICATIONS 1980 to 1984	each DM 16.00	each DM 4.50

Reduced prices for elder copies

Individual copies out of elder, incomplete volumes, as long as stock lasts:

2/1971 * 1, 2, 4/1972 * 2, 4/1973 * 1, 3/1974 * 1, 2 , 3, 4 /1975,	**each DM 2.00**
2, 3, 4/1976 * 1, 2, 4/1977 * 1, 2/1978 * 1, 2, 3/1979	**each DM 2.00**
Plastic binder for 3 volumes	DM 10.00

All prices including surface mail

When ordering 3 complete volumes, a free binder is included!

UKWberichte T. Bittan OHG · Jahnstr. 14 · Postfach 80 · D-8523 Baiersdorf
Tel. 09133-47-0 · Telefax 09133-4747 · PSchKto Nürnberg 30455-858